DEGREE PROJECT FOR MASTER OF SCIENCE WITH SPECIALIZATION IN ROBOTICS
DEPARTMENT OF ENGINEERING SCIENCE
UNIVERSITY WEST

Design and simulation of hanger automation for used garments

Kande Durayalage Gayan Asanka Rathnayaka

A THESIS SUBMITTED TO THE DEPARTMENT OF ENGINEERING SCIENCE

IN PARTIAL FULFILMENT OF THE REQUIREMENTS FOR THE DEGREE OF

MASTER OF SCIENCE WITH SPECIALIZATION IN AI AND AUTOMATION

AT UNIVERSITY WEST

2026

Date:	August 31, 2026
Author:	Kande Durayalage Gayan Asanka Rathnayaka
Examiner:	Mahmood Khabbazi
Advisor:	David Stjern
Programme:	Master Programme in AI and Automation
Main field of study:	Automation with a specialization in AI
Credits:	120 Higher Education credits (see the course syllabus)
Keywords:	Automated Garment Handling, Deformable Object Manipulation, Computer Vision, Used Clothing Recycling, Intelligent Hanging Systems
Template:	University West, IV-Master 2.10
Publisher:	University West, Department of Engineering Science S-461 86 Trollhättan, SWEDEN Phone: + 46 520 22 30 00 Fax: + 46 520 22 32 99 Web: www.hv.se

Summary

Automated sorting and inspection of used garments is increasingly important for textile reuse and recycling, yet garment handling remains difficult to automate because of fabric deformability. Placing garments onto hangers or inspection fixtures therefore continues to require significant manual intervention. This thesis investigates the design and simulation of an automated garment-hanging system using Design for Automation principles. The objective was to determine how hanger geometry and mechanical constraints could simplify garment handling while providing suitable presentation for image-based analysis. The work focused on garment surface exposure, blind insertion through the neckline, and transformation from a compact insertion state to a larger supporting configuration.

Several garment-support geometries were evaluated to study their influence on surface visibility and observation quality. Increasing the separation between the front and rear garment surfaces reduced folds and self-occlusion, while excessive volume reduced observation quality because more surface regions were viewed at unfavorable angles. Based on this trade-off, a hybrid supporting geometry was developed. A deployable hanger was then designed to address the conflicting requirements of insertion and final garment support. The hanger remains compact during neckline insertion and expands afterward to provide greater shoulder support and three-dimensional surface separation. Different insertion geometries were evaluated under translational and rotational variation to assess tolerance to positioning uncertainty.

The experiments also showed that variation in garment pickup changes the position and configuration of the neckline. Temporary front and back grippers were therefore introduced to mechanically open and stabilize the neckline before insertion, improving insertion robustness and reducing the need for configuration-specific corrections.

The individual functions were integrated into a complete hanger-cycle simulation including garment suspension, neckline preparation, compact insertion, mechanical deployment, and final garment support. Additional trials with different upper-body garments indicated that the concept can operate across a practical range of garment sizes, while smaller garments and narrow neckline or internal dimensions remain limiting cases.

Overall, the study demonstrates that mechanical geometry and controlled garment constraints can reduce uncertainty in automated garment hanging. The proposed combination of active neckline control, compact insertion geometry, and deployable garment support provides a feasible simulation-based approach for upper-body garment handling. Physical validation is still required to evaluate textile behavior, gripping performance, actuator requirements, cycle time, and robustness across a wider range of garments.

Preface

This master's degree report, Design and simulation of hanger automation for used garments, was written as part of the requirements for the Master of Science with specialization in AI and Automation at University West. The research addresses the real-world complexities of automated textile handling and was heavily inspired by the operational processes and photo-tunnel technologies implemented at Wargön Innovation.

I would like to express my sincere gratitude to my advisor, David Stjern, for his continuous guidance, insights, and support throughout the development of this project. I would also like to thank my examiner, Mahmood Khabbazi, for his constructive feedback and academic oversight. Finally, I extend my appreciation to Wargön Innovation for providing the practical context and industrial inspiration that made this research possible.

Finally, I would like to thank my wife Nisadi Wickramaseka for her patience, encouragement, and continuous support throughout my studies and the completion of this thesis.

Affirmation

This master's degree report, *Design and simulation of hanger automation for used garments*, was written as part of the master's degree work needed to obtain a Master of Science with specialization in Robotics degree at University West. All material in this report, that is not my own, is clearly identified and used in an appropriate and correct way. The main part of the work included in this degree project has not previously been published or used for obtaining another degree.

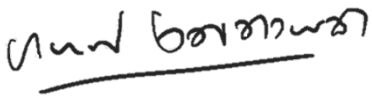

Signature by the author

08/31/2026

Date

Kande Durayalage Gayan Asanka Rathnayaka

Contents

SUMMARY ..... **III**

PREFACE ..... **IV**

AFFIRMATION ..... **V**

CONTENTS ..... **VI**

SYMBOLS AND GLOSSARY ..... **VIII**

Main Chapters

1 INTRODUCTION **1**

1.1 BACKGROUND 1
1.2 PROBLEM DESCRIPTION 1
1.3 AIM 2
1.4 RESEARCH QUESTIONS 2
1.5 LIMITATIONS 2

2 RELATED WORK (BACKGROUND) **3**

2.1 CHALLENGES IN TEXTILE MANIPULATION 3
2.2 PERCEPTION AND GRASP POINT LOCALIZATION 4
2.2.1 Semantic Landmarks and Kinematic Constraints *4*
2.2.2 End-Effectors and Tactile Feedback *4*
2.3 INDUSTRIAL APPROACHES TO THE GARMENT HANGING. 4
2.4 DESIGN FOR AUTOMATION (DFA) 5
2.4.1 Self-Centring Geometry and Lead-in Features *5*
2.4.2 Passive Compliance for Material Safety *6*
2.4.3 Constraint of Degrees of Freedom (DoF) *6*
2.4.4 Transitioning Toward Blind Insertion *6*

3 METHOD **7**

3.1 PROBLEM DEFINITION AND REQUIREMENT FORMULATION 7
3.2 CONCEPT GENERATION 7
3.3 CONCEPT SELECTION 8
3.4 PROTOTYPE DEVELOPMENT 8
3.5 TESTING AND EVALUATION 8
3.6 METHODOLOGICAL RATIONALE 9

4 SYSTEM DEVELOPMENT AND EXPERIMENTAL SETUP **10**

4.1 PROBLEM DEFINITION AND REQUIREMENTS 10
4.2 SIMULATION AND REFINEMENT 10
4.3.1 The Quality Coefficient Calculation *10*
4.3.3 Performance Metrics *11*
4.4 CAMARA ANGLE SELECTION 12
4.5 INITIAL HANGER GEOMETRY IDEA GENERATION 13
4.5.1 Baseline: Standard Hanger *13*
4.5.2 Industrial Benchmarks: Mannequins *14*

4.5.3 Experimental Inspiration: Hanger1 ..... *14*
4.5.4 Inflatable Geometries *15*
4.6 KPI Result of the initial geometries 16
4.6.1 Weighted Optimization *17*
4.7 Conclusion for the Next Phase of Development 20
4.8 Validation of the Hybrid Geometry 20
4.9 Development of the Deployable Hanger Concept 21
4.10 Blind-Insertion Simulation and Evaluation 23
4.10.1 Experimental Setup *23*
4.10.2 Evaluation of Garment-Pickup Variation *26*
4.10.3 Pickup-Variation Results *28*
4.10.4 Active Mechanical Control of the Neckline Opening *28*
4.10.5 Active-Opening Result *29*
4.10.6 Full Hanger-Cycle Simulation *30*
4.10.7 Modified shoulder-deployment sequence *32*
4.10.8 Evaluation of different size of garments *32*

5 RESULTS AND DISCUSSION 35

5.1 Influence of Supporting Geometry on Surface Exposure 35
5.2 Observation Quality and the Influence of Geometry 35
5.3 Influence of the Number of Cameras 36
5.4 Saliency-Weighted Evaluation 36
5.5 Selection of the Hybrid Geometry 36
5.6 Validation of the Hybrid Geometry 37
5.7 Full Hanger-Cycle Simulation 37
5.7.1 Active neckline control and insertion geometry *37*
5.7.2 Staged deployment of the hanger *39*
5.8 Discussion in Relation to Research Questions 40
5.8.1 Research Question 1: Surface Exposure and Observation Quality *40*
5.8.2 Research Question 2: Blind Insertion and Deployable Hanger Geometry *41*
5.8.3 Research Question 3: Advantage Over the Conventional Hanger *42*
5.8.4 Research Question 4: Automation Efficiency and Hanging Success *42*
5.9 Limitations of the Evaluation 43
5.9.1 Cloth Material Representation *44*
5.9.2 Contact and Penetration Limitations *44*
5.9.3 Simplified Collision Geometry *45*
5.9.4 Gripping and Attachment Idealization *45*
5.9.5 Limited Garment Variation *45*
5.9.6 Simulation and Physical Cycle Time *46*
5.9.7 Implications for Physical Validation *46*

6 CONCLUSION 47

6.1 Future Work and Research 48
6.2 Critical Discussion 49
6.3 Generalization of the Results 50

7 REFERENCES 51

Symbols and glossary

CDO	Cloth-like Deformable Object. Textiles characterized by infinite degrees of freedom, complex nonlinear dynamics, and a lack of a defined rigid shape.
DfA	Design for Automation. An engineering methodology focused on designing products specifically to facilitate easy and efficient automated handling.
DO	Deformable Object. Objects that do not maintain a stable shape during interaction, complicating traditional rigid-body manipulation.
DOF	Degrees of Freedom. The number of independent parameters that define a system's configuration.
SMA	Shape Memory Alloy. A type of material used in spring-actuated clamps for reconfigurable passive hangers.
USD	Universal Scene Description. A scene-description format used for representing simulation assets, including garments and mechanical components.
Isaac Sim	A robotics simulation environment used in this study for deformable-garment interaction, blind insertion, and full hanger-cycle simulation.
CCD	Continuous Collision Detection. A collision-handling method used to reduce the possibility of fast-moving simulated components passing through other objects between physics updates.

1 Introduction

The global secondary textile market has entered a period of rapid industrialization, driven by the dual pressures of environmental sustainability and the massive throughput requirements of the circular economy. The traditional reliance on manual visual assessment for the grading of used apparel has proven increasingly unsustainable due to inherent human limitations, including fatigue, visual strain, and subjectivity[1], [2]. To achieve consistency and scalability, industry is transitioning toward automated systems that integrate high-resolution imaging, specialized lighting, and deep learning architectures. When transitioning toward automated systems, key change is the handling of the garments. Unlike rigid industrial components, garments are Cloth-like Deformable Objects (CDOs) with infinite degrees of freedom, complex nonlinear dynamics, and frequent self-occlusion.

1.1 Background

Wargön Innovation (WI) has made strides in this area by implementing a photo-tunnel designed to capture high-quality images for AI-driven garment analysis and redirection. While the photographing and analysis stages are increasingly automated, a significant manual bottleneck remains: the process of placing individual garments onto hangers. Current automated sorting lines are limited by the need for human intervention at this stage, which reduces overall throughput and increases operational costs.

1.2 Problem Description

The automated handling of flexible textiles remains one of the most significant hurdles in modern robotics. Traditional garment hangers are designed exclusively for human ergonomics, relying on the high-degree-of-freedom dexterity and tactile feedback of human hands. Replicating these "fine-motor" actions in a robotic system requires prohibitive computational power for real-time motion planning and high-precision visual servoing.

Furthermore, industrial hanger design has historically prioritized low-cost manufacturability and retail display aesthetics over robotic compatibility. These hangers often lack defined "pick-points," are prone to nesting (tangling) in bulk, and do not ensure the garment is presented in a consistent orientation for AI-based vision analysis.

To bridge the gap between bulk textile collection and automated sorting, this project proposes a shift toward hardware-centric uncertainty management. By applying Design for Automation (DfA) principles, specifically Mechanical Constraint Programming the hanger is transformed from a passive tool into an active guide for the robotic manipulator[3].

The core objective is to facilitate blind robotic operation: rather than relying on high-latency, sensor-heavy 'search and hang' algorithms, the hanger's geometry features self-aligning lead-ins and standardized grasping interfaces. These physical constraints funnel the manipulator into the correct position, reducing a complex, multi-axis spatial problem to a repeatable, low-complexity linear operation.

1.3 Aim

The purpose of this project is to develop an automated method for handling upper-body garments that maximizes both operational efficiency and garment surface exposure for AI analysis. By applying DfA principles, this research investigates how redesigned hanger geometries can simplify the robotic insertion process.
The specific aims of this project include:

- Identifying and designing innovative hanger geometries that facilitate "blind" robotic insertion.
- Evaluating these designs to ensure they maintain the garment's natural shape for accurate AI analysis.
- Developing a simulated prototype to demonstrate the interaction between the garment and the redesigned hanger system.

1.4 Research Questions

To achieve these aims, the project seeks to answer the following questions:

1. How can hanger geometry be modified to maximize surface exposure for AI analysis?
2. How can hanger geometry be modified to allow for "blind" robotic insertion while maintaining the garment's natural shape?
3. Does a specialized hanging fixture provide significantly better surface area exposure compared to a standard hanger?
4. Which automation approach yields the best efficiency and success rate for garment hanging?

1.5 Limitations

This study focuses specifically on the hanging process and does not cover the downstream AI analysis or the hardware within the photo tunnel. Initial testing will involve garments presented on flat or semi-structured surfaces rather than tangled bulk textiles. Furthermore, the scope is restricted to common upper-body garments that do not fully open in the middle.

2 Related work (Background)

The automated handling textiles represent a significant frontier in robotics, characterized by the inherent difficulty of managing deformable objects (DOs) with infinite-dimensional state spaces and unpredictable, non-linear dynamics[4], [5], [6].This "limpness" makes traditional rigid-body manipulation strategies ineffective, as textiles do not maintain a stable shape during interaction[7], [8]. The primary hurdle in textile robotics is the lack of a defined shape, which complicates robust and reliable grasping without damaging high-quality materials. Manual labour remains dominant in the industry because human workers can naturally identify important parts and navigate complex topological patterns, such as openings and seams. But traditional visual inspection is also limited by human fatigue and inconsistency, driving the need for automated alternatives[9], [10].

This automation challenge consists of four sub challenges. Grasping the garment, manipulation of the garment, put garment on a hanger/fixture for photographing and pass into the next process. Apart from that variability add by design also need to handle. Garment handling in laundry industry has evolved from full manual operations to fully automatic solutions. But putting garments into hanger only evolved up to semi-automated level. "MetriQ" - loading station for handling garments and Lobster hanger by JENSEN AG Burgdorf is one of the available solutions to garment loading[11]. Putting garments on a hanger is still on research level due to nature of the cloth.

2.1 Challenges in Textile Manipulation

Textile manipulation and hanging present multifaceted challenges that stem primarily from the inherent physical properties of deformable materials. A fundamental difficulty lies in the infinite dimensionality of the state space and the complex dynamics of fabric, which complicate traditional modelling and state estimation. Research in robotic garment manipulation has undergone a significant paradigm shift, transitioning from traditional quasi-static techniques toward more efficient dynamic and interactive strategies.

Early methodologies primarily relied on quasi-static actions, such as precision pick-and-place and surface-based dragging, which utilize friction between the garment and a workspace to manage fabric deformability. While these approaches offer high precision for alignment and folding tasks, they are often characterized by low operational efficiency that requiring numerous interactions to resolve severely crumpled states[5]. To address these limitations, dynamic manipulation paradigms, exemplified by systems such as FlingBot, leverage high-velocity "flinging" primitives to exploit the garment's own mass and momentum[12]. These methods effectively unfurl cloth in fewer steps and expand the robot's functional reach beyond its static kinematic limits.

Concurrently, the interactive perception paradigm suggests that manipulation and perception must be deeply coupled to resolve occlusions; in this framework, exploratory movements are used to reveal hidden functional boundary components, such as necklines and sleeves, that are not visible in static, flattened configurations[8]. Recent advancements have further integrated these paradigms with large-scale simulated environments and datasets like ClothesNet, facilitating the development of robust, data-driven policies that generalize across diverse garment categories and complex physical states[13], [14]. Accomplishment of the successful manipulation of garments depends on the grasping garments.

Identifying where to grasp a garment is critical for successful manipulation. To achieve successful interaction, research focuses on the intersection of advanced computer vision for point identification and specialized end-effector design. However there no commercially used specified garment grasping grippers in the market.

2.2 Perception and Grasp Point Localization

The identification of optimal grasping points is the primary hurdle in transforming a limp mass of fabric into a structured form. This process generally divided into the detection of geometric features and semantic key points. Geometric strategies, often developed through self-supervised learning frameworks like FlingBot, prioritize corners and edges as the most efficient points for unfolding operations[12]. In more complex tasks, such as the manipulation of headwear or garments with openings, systems identify "boundary components" the closed contours of apertures. By analyzing these contours for regions of low curvature, robots can determine where a gripper can most effectively penetrate the opening without snagging[8]. Furthermore, semantic segmentation models now categorize fabric at the pixel level, distinguishing between "inner edges," "outer edges," and "corners" to provide a granular map for robotic path planning[4].

2.2.1 Semantic Landmarks and Kinematic Constraints

Beyond basic geometry, the use of semantic landmarks is essential for high-level tasks such as automated folding, sizing, hanging and inspection. These systems target specific anatomical points on a garment, including collars, sleeve midpoints, armpits, and hems. In the context of automated sizing, these landmarks serve as vertices for calculating precise dimensions from three-dimensional point cloud data. The execution of a "pinch-grasp" at these points requires the robot to account for local fabric topology; for instance, aligning the gripper parallel to small creases increases the probability of a stable grasp. In dual-arm configurations, these grasp points are further constrained by kinematic planning to prevent mechanical singularities, arm crossovers, or self-collision[12].

2.2.2 End-Effectors and Tactile Feedback

The physical interaction with textiles necessitates a departure from standard rigid-body grippers. Modified industrial grippers often incorporate high-friction elastomeric tips or foam layers to increase the contact area and prevent fabric slippage[12]. For "pick-and-place" operations from flat surfaces, vacuum-based pickers utilize fan-driven suction and compliant rings to lift single layers of fabric without inducing mechanical damage[7]. More advanced research explores soft grippers and high-DOF anthropomorphic hands, such as the Shadow Dexterous Hand, which utilizes 20 degrees of freedom to mimic human dexterity[8]. To close loop control, these grippers are increasingly integrated with tactile-reactive technologies like GelSight and BioTec tactile sensor which allow the system to estimate the fabric's pose and frictional forces through real-time "touch" feedback[4].

2.3 Industrial approaches to the garment hanging.

Apart from the deformability of the textile, design variation is another factor that making automating the hanging process even difficult. Main challenge lies on finding common starting point for stating hanging process. Available hangers are design to insert from the neck opening(neckline). Neckline varies depending on the size and the fashion design. Current industrials solutions like Lobster hanger shows in the Figure 1 by JENSEN AG Burgdorf

Figure 1 Lobster hanger by JENSEN AG Burgdorf

sort this problem up to semi-automated level by allowing multiple configurations to hang garments [15]. Achieving full autonomy remains a primary focus of research.

In some industrial workflows, the "gripper" is replaced by a specialized hanging system such as Reconfigurable Passive Hangers[7] and Smart Robotic Hangers.

- Reconfigurable Passive Hangers: These consist of three articulated fingers with SMA (shape memory alloy) spring-actuated clamps. A robot "sets" the hanger by dragging its fingers to specific points on a fabric panel before locking them.
- Smart Robotic Hangers: Designed as multi-link robotics, these devices extend into the interior of a garment and stretch it taut from the inside to facilitate automated inspection for workmanship defects and shade variations.

2.4 Design for Automation (DfA)

While existing research focuses heavily on sensor-driven algorithms and complex multi-DOF (degree-of-freedom) robotic control to manage uncertainty, there is a noted gap in hardware-centric solutions. As identified in the problem description, traditional hangers prioritize human ergonomics and aesthetics over robotic compatibility. A shift toward Mechanical Constraint Programming where the physical geometry of the hanger guides the robotic manipulator represents a novel approach to simplifying the "search and hang" task into a repeatable linear operation, thereby reducing the computational overhead for real-time motion planning.

2.4.1 Self-Centring Geometry and Lead-in Features

A primary hurdle in textile hanging is the spatial uncertainty of the garment after the initial pick-up. Even with advanced grasping strategies like FlingBot[12], the exact orientation of a neckline or sleeve may vary by several centimetres. To compensate, DfA principles suggest the use of self-cantering geometry. By incorporating tapered "lead-in" edges or funnel-shaped profiles into the hanger's arms, the tool can physically "capture" the garment's opening. As the robot moves the hanger into the garment, these geometric constraints force the fabric to slide into a cantered, predictable pose, effectively correcting for inaccuracies in the robot's kinematic path or the vision system's initial estimate[8].

2.4.2 Passive Compliance for Material Safety

Interacting with delicate textiles requires a departure from the high-stiffness requirements of traditional rigid-body assembly. A DfA-centric tool incorporates passive compliance of the use of springs, flexures, or elastomeric materials that allow the tool to "give" upon contact[7]. This mechanical elasticity serves two purposes:

1. It prevents the tearing of high-quality fabrics by limiting the maximum force applied during insertion.
2. It eliminates the need for high-frequency, expensive force-torque sensors and closed-loop control, as the hardware inherently manages the contact forces [4].

2.4.3 Constraint of Degrees of Freedom (DoF)

Fabric is characterized by its ability to deform in nearly infinite directions, making state estimation a significant computational burden. Effective fixture design utilizes Mechanical Constraint Programming to "pin" or "stretch" the fabric, thereby reducing its Degrees of Freedom (DoF). By transitioning the garment from a crumpled 3D state to a tensioned configuration on a specialized hanger or fixture will effectively collapses the complex search space into a structured 2D manifold[7].

2.4.4 Transitioning Toward Blind Insertion

The goal of applying DfA to textile robotics is the achievement of Blind Insertion. Most current research relies on continuous visual servoing, which is often hampered by self-occlusions and human-like fatigue in visual processing. By leveraging self-aligning geometry and mechanical constraints, the hanging process can be transformed into a "blind" linear operation. Once the robot identifies a common starting point, the physical properties of the hanger guide the rest of the task. This reduces the computational overhead required for real-time motion planning and increases the operational speed, bringing robotic textile handling closer to the efficiency levels of manual labor.

3 Method

The research methodology for this thesis is structured around the Engineering Design Process (EDP)[16], which serves as the overarching framework for navigating the complexities of automating deformable object manipulation. The EDP is selected because its iterative nature allows for the systematic translation of high-level industrial problems into quantifiable mechanical requirements and validated technical solutions. Engineering Design Process (EDP) selected for its structured yet inherently iterative nature, which is particularly well-suited to addressing complex and ill-defined ("wicked") engineering problems where the solution space is not initially clear [17]. Rather than following a linear project plan, the EDP provides a requirement driven logic that begins with rigorous problem definition and requirement formulation, ensuring that the garment hanger automation design is guided by the functional demands of a circular economy such as high-throughput processing and compatibility with AI-driven analysis rather than conventional, human-centered design considerations. Furthermore, the EDP supports systematic uncertainty management, which is critical given the infinite degrees of freedom associated with cloth-like deformable objects (CDOs). This enables the integration of Design for Automation (DfA) principles and mechanical constraint programming during concept generation, facilitating a strategic shift from computationally intensive, vision-based control toward hardware-oriented, "blind" insertion methods that reduce latency.

The application of this methodology is divided into the following logical phases: problem definition and requirement formulation, concept generation, concept selection, prototype development, and testing and evaluation. Each phase produces outputs that are used as input to the next phase, allowing the design to be refined in an iterative manner.

3.1 Problem definition and requirement formulation

The first phase defines the engineering problem addressed in the thesis. The main challenge is the manual garment-hanging step in the sorting workflow at Wargön Innovation, where a flexible garment must be positioned on a hanger before image-based analysis can take place. Based on the problem description and the intended application context, the functional requirements of the system are defined through a structured mind-mapping process. This visual approach allowed for a comprehensive breakdown of the problem and helped to identify the area needs to be researched.

These requirements focus on three main aspects. First, the hanger system should maintain the garment in a stable and repeatable position. Second, it should maximize garment surface exposure for later AI-based inspection. Third, it should support robotic handling with minimal reliance on complex sensing and motion planning. In addition to the functional requirements, constraints such as manufacturability, simplicity, and compatibility with the intended sorting environment are also considered.

3.2 Concept generation

In the second phase, alternative concepts are generated for the automated hanging system. Rather than treating the hanger as a passive retail object, the concepts are developed according to Design for Automation (DfA) principles, where the geometry of the hanger is

used to support the robot during insertion and positioning. The main objective of this phase is to identify geometries that can guide the garment into the correct position through physical interaction rather than through continuous visual correction.

The concept generation process includes ideas related to self-cantering features, lead-in geometry, passive compliance, and fixture-based constraint of the garment opening. Multiple variants are created for comparison, and each concept is checked against the established requirements. At this stage, the output is a set of candidate hanger designs and system configurations.

3.3 Concept selection

The third phase evaluates the candidate concepts using predefined selection criteria. The purpose of this phase is to choose the most promising design for further development. The selection criteria are based on the research aim and the practical constraints of the system.

The main evaluation criteria include:

- ability to support blind or low-complexity robotic insertion,
- ability to keep the garment in a natural and open configuration,
- expected improvement in surface exposure for image analysis,
- mechanical simplicity and feasibility of implementation,
- tolerance to variation in garment size and shape.

Each concept is compared against these criteria and ranked accordingly. The selected concept is the one that best balances automation potential, garment presentation quality, and design feasibility.

3.4 Prototype development

After concept selection, a prototype of the chosen hanger geometry is developed in a simulation environment. The purpose of the prototype is not only to visualize the design, but also to evaluate whether the proposed design can support the intended garment interaction. The prototype is developed as a simplified representation of the real system so that the influence of design and constraint strategy can be studied in a controlled way.

This phase includes defining the geometric parameters of the hanger, modelling the garment interaction, and setting up the simulation conditions used for evaluation. The prototype is therefore a tool for evaluating the design logic of the concept rather than a final industrial product.

3.5 Testing and evaluation

The final phase consists of simulation-based testing and evaluation of the prototype. The tests are used to assess whether the design satisfies the functional requirements defined earlier in the method. The results are evaluated quantitatively, with attention to how well the proposed system supports garment placement, garment stability, and surface exposure.

The evaluation compares the proposed design with the expected performance of a conventional method currently practice in Wargön Innovation. The results are then used to refine the design and to determine whether the concept offers a meaningful improvement for automated garment handling. This final evaluation forms the basis for the discussion of the research questions and the conclusions of the thesis.

3.6 Methodological rationale

The EDP is selected because this thesis addresses a practical engineering problem with several possible solutions and no single predefined answer. A linear implementation approach would not be suitable, because the design must be explored, compared, and refined before a final concept can be justified. The EDP provides a structured way to move from problem identification to verified design output.

The use of simulation is also justified because it allows the interaction between garment and hanger geometry to be studied before physical prototyping. This is particularly important in textile handling, where garment behavior is difficult to predict and where repeated physical trials may be costly or time-consuming. Simulation therefore supports early-stage validation of design logic and reduces the risk of developing a concept that is impractical in reality.

4 System Development and Experimental Setup

The investigation for this research was conducted following the Engineering Design Process (EDP)[16], utilizing a quantitative approach through simulation-based experimentation. To effectively address the complexities of automated garment handling, the proposed solution is developed systematically and divided into three distinct operational modules. The methodology is executed in the following chronological phases, structured to provide a clear, objective progression of the work rather than a chronological diary of activities.

4.1 Problem Definition and Requirements

The initial phase involves a holistic definition of the technical gap at Wargön Innovation, specifically focusing on the bottleneck of manual garment hanging. To address this, functional requirements were established with a primary focus on maximizing surface area exposure for AI analysis and ensuring the system's compatibility with the existing photo-tunnel. Following this, a literature review was conducted to identify state-of-the-art techniques in Cloth-like Deformable Object (CDO) manipulation. This review specifically research "Design for Automation" (DfA) principles to better understand how modifying hanger geometry can simplify robotic grasping and insertion compared to standard, human-centric hangers.

4.2 Simulation and Refinement

- The screened designs were subjected to simulated experimentation.
- The quantitative results gathered from these simulations were utilized to iteratively refine the mechanical designs, particularly the hanger geometry and the robotic interaction parameters.

4.3 Baseline Establishment & Evaluation Framework

To objectively evaluate the efficiency of a camara rig, a binary "coverage" check (whether a pixel is seen or not) is insufficient. In photogrammetry, data quality is a function of the Frustum Effect the geometric distortion that occurs when a camera captures a surface at an acute angle[18]. This research establishes a Quality-Weighted Matrix (QWM) approach. This matrix maps 3D geometric integrity onto 2D UV space, providing a standardized baseline to compare different garment geometries.

4.3.1 The Quality Coefficient Calculation

For each camera C_i, the quality Q of a surface face f is calculated based on the Lambertian cosine law as show in the Figure 2:

$$Q = \left| \overrightarrow{N_f} . \overrightarrow{D_{Ci}} \right|$$

Where:

$\overrightarrow{N_f}$ is the surface normal of the face.

$\overrightarrow{D_{Ci}}$ is the normalized direction vector from the camera to the face center.

A value of 1.0 (Pure White) represents a perfect perpendicular capture (maximum resolution), while values approaching 0.0 (Black) represent extreme grazing angles where the pixel data is stretched and unusable. This formulation is widely used in computer graphics and vision to model surface visibility and shading[19].

4.3.2 Reference Standards

To evaluate the results, three distinct maps are generated for the baseline:

1. **Individual Angle Maps:** Used to identify "Blind Spots" inherent to specific camera heights or angles.
2. **The Master Quality Map (Integrated Best-View):** A pixel-wise maximum composite of all 4 angles. This map represents the best achievable observation quality for each UV coordinate under the given camera configuration and serves as an upper-bound performance reference for the geometry.

3. **The Ground Truth (Ideal Reference):** A binary map representing the total UV area occupied by the garment. This acts as the "Denominator" for efficiency calculations.

4.3.3 Performance Metrics

The effectiveness of the design transition from the Standard Hanger (baseline) to the modified geometry is evaluated using the following Key Performance Indicators (KPIs):

4.3.3.1 Surface Coverage

Measures the proportion of the garment surface that is visible from at least one camera, reflecting the system's ability to minimize occlusions.

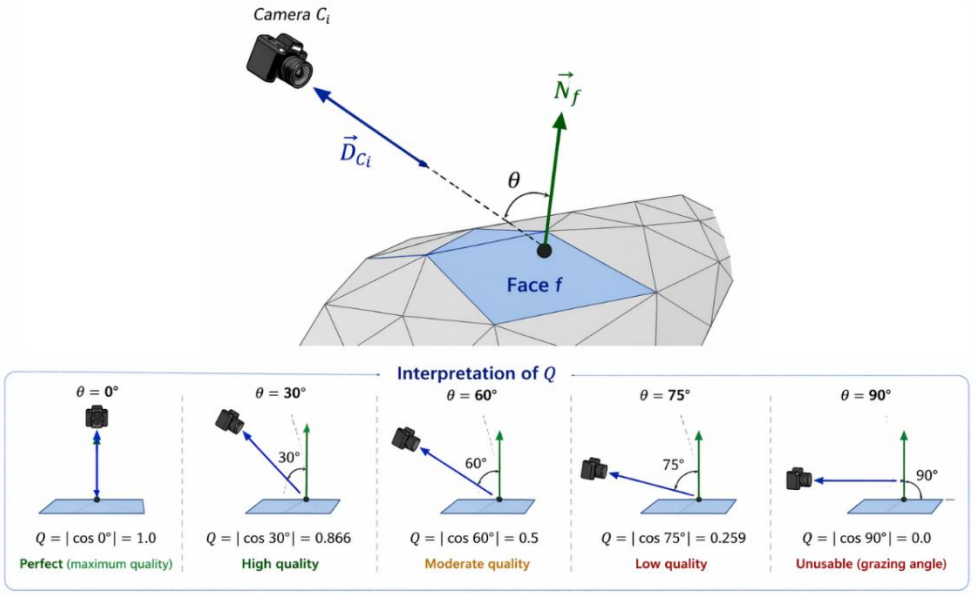

Figure 2 Effect of viewing angle on surface quality using Lambert's cosine law

$$Coverage = \frac{Number\ of\ pixels\ with\ Q > 0}{Total\ reference\ pixels}$$

4.3.3.2 Mean Sampling Integrity

Quantifies the average observation quality across visible regions, indicating how effectively the system reduces angular distortion and the Frustum Effect.

$$Mean\ Quality = \frac{\sum Q(u,v)}{Number\ of\ visible\ pixels}$$

4.3.3.3 System Efficiency Score

Represents the overall data quality of the system by combining both visibility and angular quality into a single metric. This serves as the final "data grade" for evaluating and comparing hanger geometries in the context of exposing the maximum area of garment.

$$Efficiency\ Score = \frac{\sum Q(u,v)}{Total\ reference\ pixels}$$

4.4 Camara angle selection

To evaluate the practical feasibility of a low-cost scanning rig, a Greedy Iterative Selection algorithm[20] was developed. Instead of manually placing cameras, the system analyzed all 64 potential viewpoints that shows in **Figure 3** and iteratively selected the 4 indices that provided the maximum cumulative Quality Coefficient Q. This approach ensures that the resulting KPI reflects the 'Best Case Scenario' for a 4-camera hardware configuration. The selection process follows a marginal-utility logic:

1. The first camera index i is selected based on the highest individual Quality Coefficient (Q) across the UV domain.
2. Subsequent cameras are selected by maximizing the marginal information gain, defined as the increase in total surface coverage not already provided by the previously selected indices. This heuristic ensures the elimination of redundant viewpoints and optimizes the spatial distribution of the camera rig. While global optimization methods (e.g., Brute Force) exist, the Greedy approach provides a near-optimal approximation (>63% of the theoretical maximum[20]) with a linear computational complexity, making it suitable for rapid prototyping of the setup.

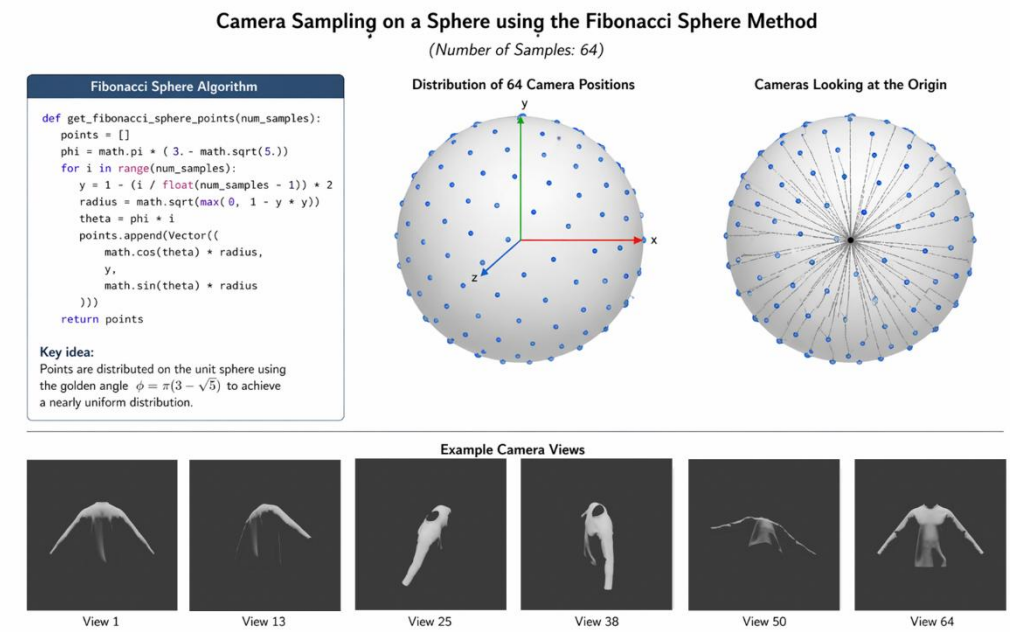

Figure 3 Camera positions generated using the Fibonacci sphere method with 64 samples.

4.5 Initial hanger geometry idea generation

The selection of support structures for this study followed an evolutionary logic, moving from industrial baselines to theoretically optimized geometries. The goal was to quantify how much the physical shape of the "hanger" dictates the surface details availability of the garments. From Figure 4 to Figure 8 represent the used support geometry and the simulated garments with the supported geometry on CLO3D.

4.5.1 Baseline: Standard Hanger

The Standard Hanger shows in Figure 4 was selected as the control group for this experiment. In many low-cost digitization workflows, garments are captured in a "flat-hang"

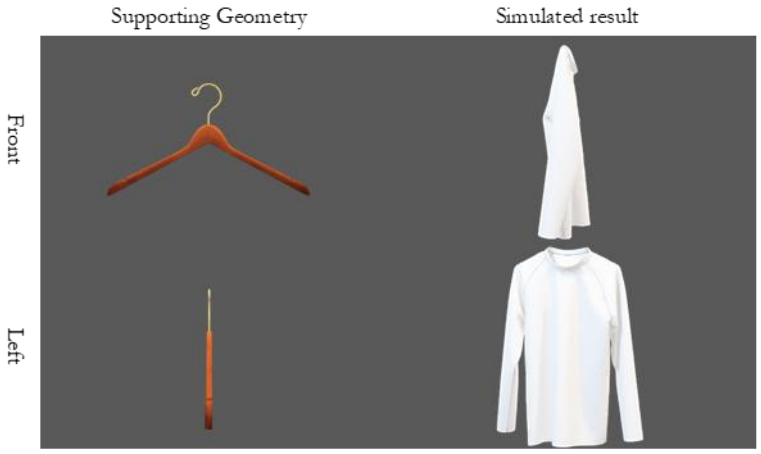

Figure 4 Standard Hanger and the simulated garment

state. This baseline represents the minimum viable setup, characterized by significant fabric overlapping and sharp folds that traditionally hinder 3D reconstruction.

4.5.2 Industrial Benchmarks: Mannequins

Mannequin 1 shows in Figure 5 and Figure 6 shows the half body mannequinsused in the fashion industry. Mannequins are widely used because they provide a 3D volume that mimics the human form, naturally reducing deep folds. These models were included to provide an upper-performance ceiling against which all other experimental designs were measured. Mannequin 3 shows in Figure 6 also used display the garments.

4.5.3 Experimental Inspiration: Hanger1

2D frame shows in Figure 7 is a specialized design derived from existing literature on garment preservation and scanning. This model was inspired by Application of smart system to textile industry: Preliminary design of a smart hanger for garment inspection[21], which suggests that by tensioning the garment can reduce occlusion. It serves as a middle ground between a simple hanger and a full mannequin.

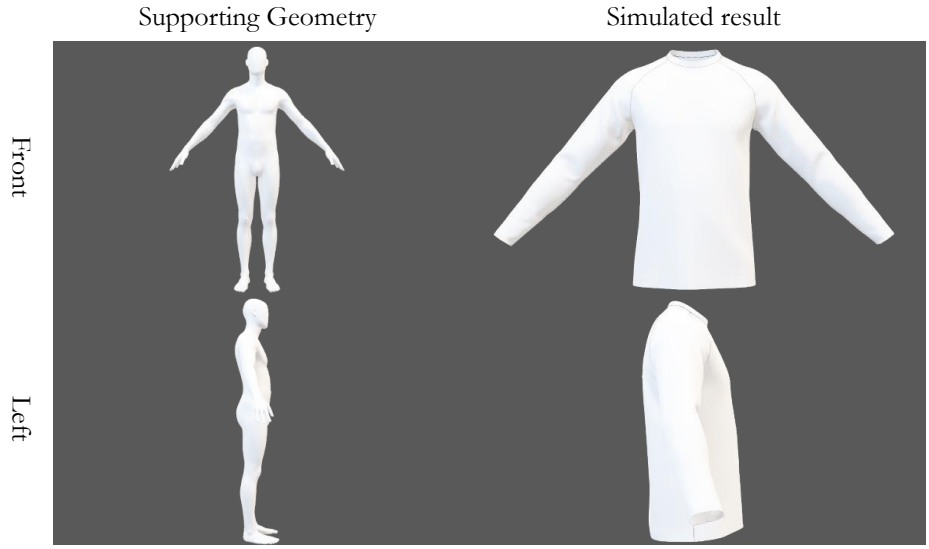

Figure 5 Mannequin 1 and the simulated garment

4.5.4 Inflatable Geometries

The Inflatable Series showed the Figure 8 constitutes the primary innovative contribution of this research, serving as a hybrid solution that bridges the gap between traditional 2D hangers and 3D mannequins. Inspired by the volumetric efficacy of mannequin-based imaging yet optimized for portability and cost-efficiency these models were subjected to a systematic sensitivity analysis across a lateral inflation gradient ranging from 10% to 100%. This approach facilitates a precise evaluation of the transition from planar to volumetric support geometries, with the ultimate objective of identifying the minimum volume threshold required to achieve 'mannequin-level' data integrity while eliminating the logistical constraints of rigid, high-bulk structures.

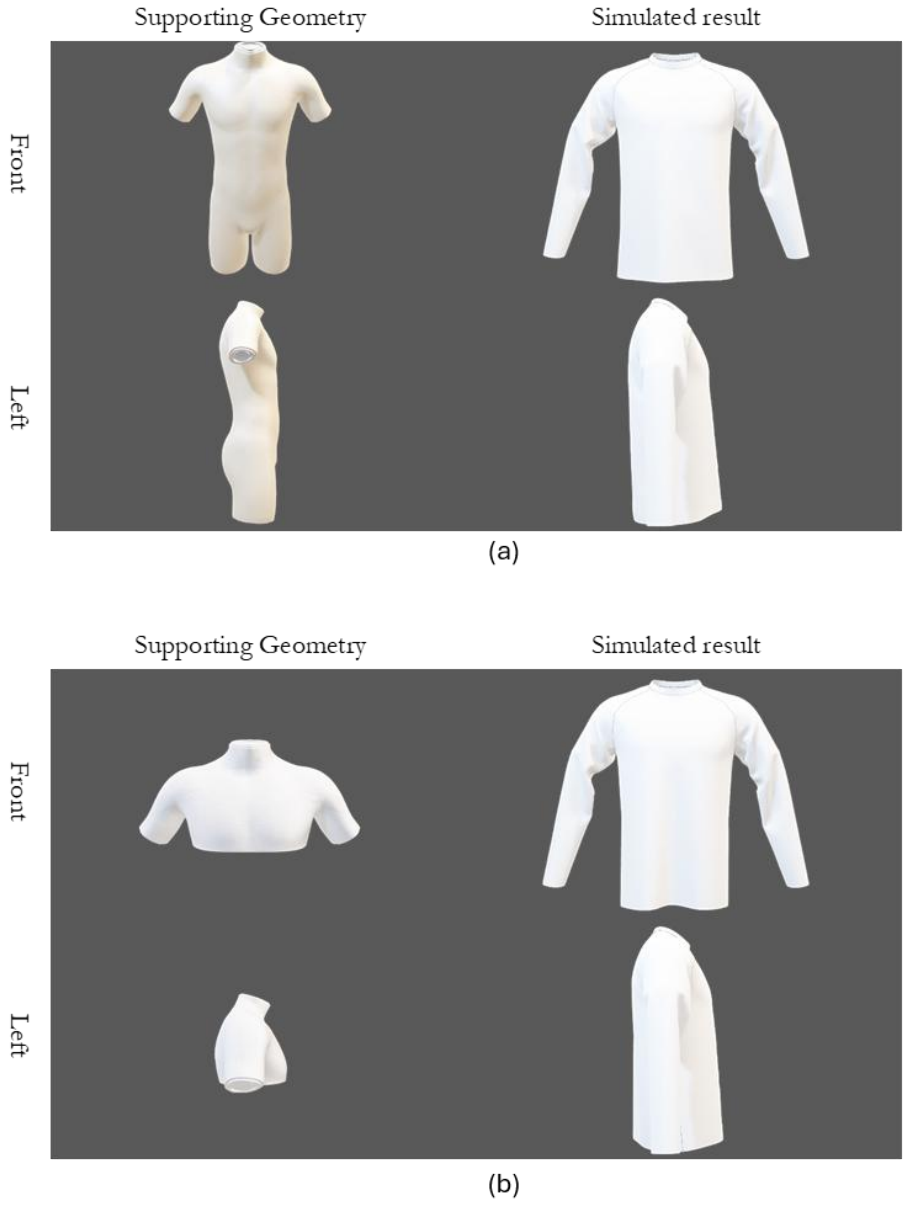

Figure 6 (a) Mannequin 2 and the simulated garment, (b) Mannequin 3 and the simulated garment

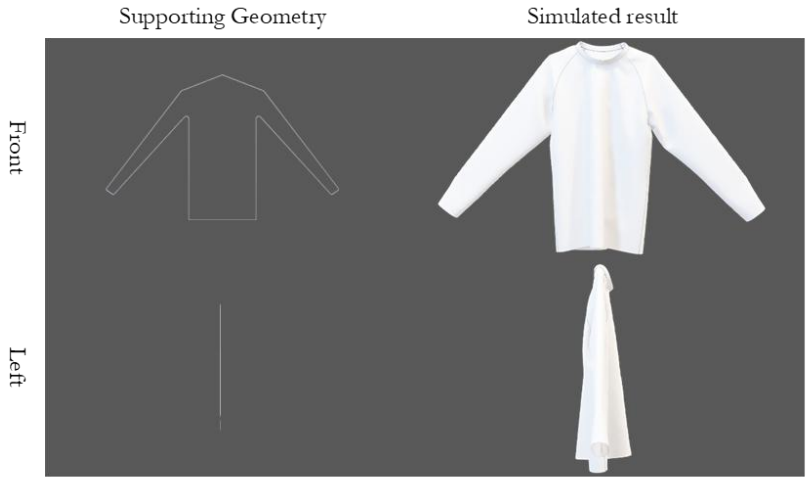

Figure 7 The 2D frame and the simulated garment

4.6 KPI Result of the initial geometries

The initial KPI calculations utilized a uniform distribution model, where every polygon on the garment surface was treated as having equal mathematical priority. In this stage, the greedy camera selection algorithm focused strictly on maximizing total surface coverage and angular quality across the entire mesh.

However, analysis of the unweighted results revealed a limitation: the algorithm prioritized total coverage at the expense of critical garment regions. To address this, a Saliency-

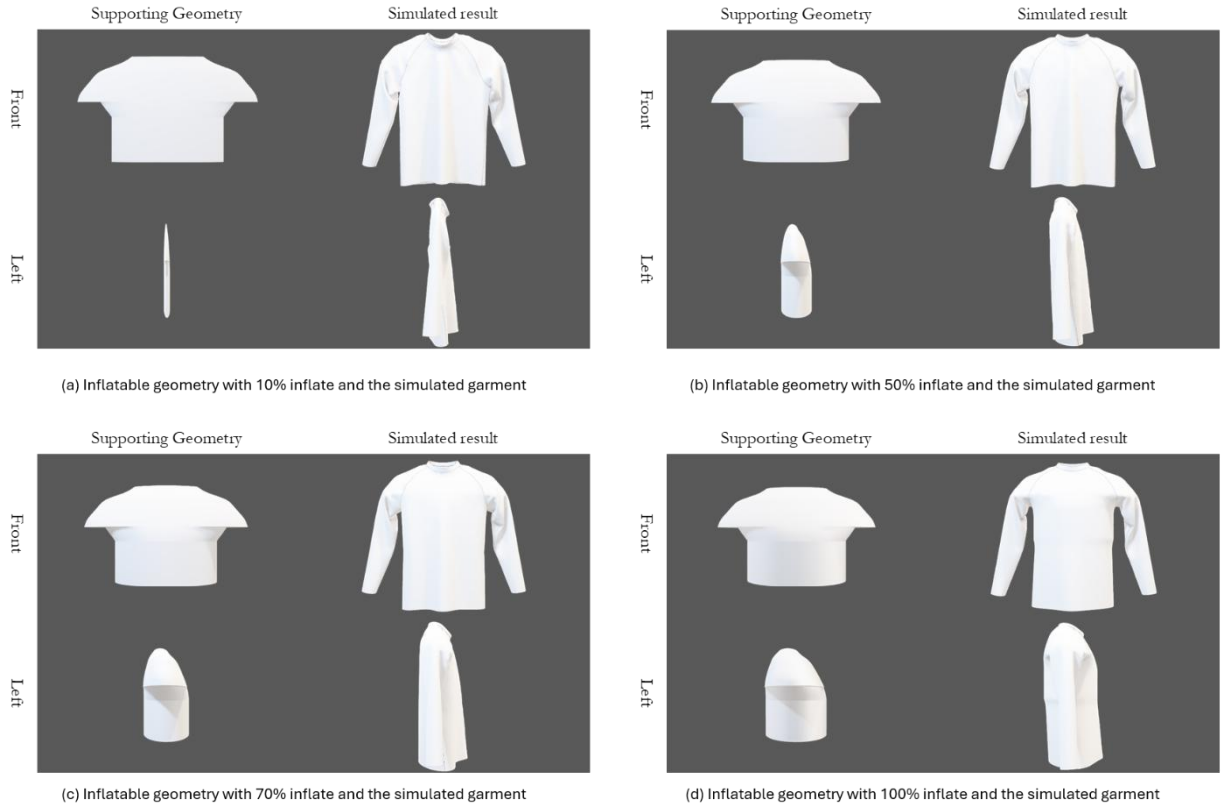

Figure 8 Inflatable geometry with inflate and the simulated garment

Weighted Reference Map was introduced into the calculation. This map was developed based on standard industrial garment defect categorization to ensure that high-priority zones areas most susceptible to defects or critical for aesthetic evaluation received greater weight during camera selection[22].

4.6.1 Weighted Optimization

To bridge the gap between raw geometric coverage and industrial utility, the greedy search algorithm was modified to include an element-wise weighting product. The selection of each camera viewpoint was determined by the Weighted Information Gain (G), defined as:

$$G = \sum((M_{new} \odot W) - (M_{current} \odot W))$$

Where:

- M: The angular quality map of the garment.
- W: The Normalized Saliency Map (derived from the industry-standard defect zones).
- $\odot$: The element-wise multiplication operator.

By integrating this weighting factor, the algorithm was forced to prioritize the "Value Zones" (such as the chest and shoulder seams). This ensures that the System Efficiency Score reflects the data quality of the areas most critical for defect detection, rather than simply maximizing the visibility of non-critical areas like the lower hem or inner sleeves. Used UV maps are showing in the Figure 9. Fallowing camara angles give the best result for most of the test geometries. Sample views in Figure 10 are representing the simulated garment on Mannequin 1.

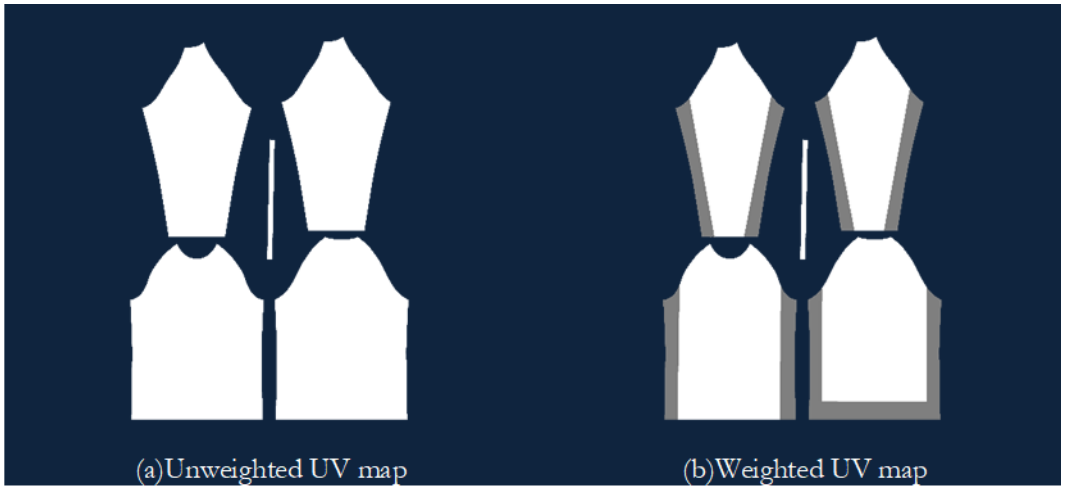

Figure 9 Reference UV maps used for the calculations

Figure 10 Render views of simulated garment on Mannequin 1

The experimental result for coverage shows in the Figure 11 demonstrate garment surface coverage across various geometries and camera configurations. A critical performance jump is observed when moving from a single-camera setup to a two-camera configuration, which effectively doubles the initial visibility across all models. By the 4-camera threshold, most of the redesigned geometries, specifically the "Mannequin" and "Inflatable" series achieve surface exposure exceeding 97%, with Mannequin 1 reaching a peak coverage of 99.35%. Beyond 4 cameras, the data indicates a plateau effect where adding additional sensors (6 or 8 cameras) results in marginal gains of less than 1%, suggesting that a 4-camera setup is the practical limit for surface exposure.

The data presented in Figure 13 highlights the precision and clarity of the surface data relative to geometric complexity. Unlike coverage, mean quality scores exhibit a more steady, linear improvement as more camera angles are added, which helps mitigate occlusions caused by the hanger's structure. The 2D frame consistently maintains the highest quality scores, such as 0.8743 in the 4-camera setup, because its low profile minimizes self-shadowing. Conversely, while high-volume volumetric geometries (Inflatable 10% to 100%) achieve high surface visibility, there is a measurable decline in the mean quality scores as the volume increases. This suggests that although the cameras can "see" the entire surface area, the density of useful data points or pixels per unit of area decreases as the surface expands and curves away from the sensor's focal plane.

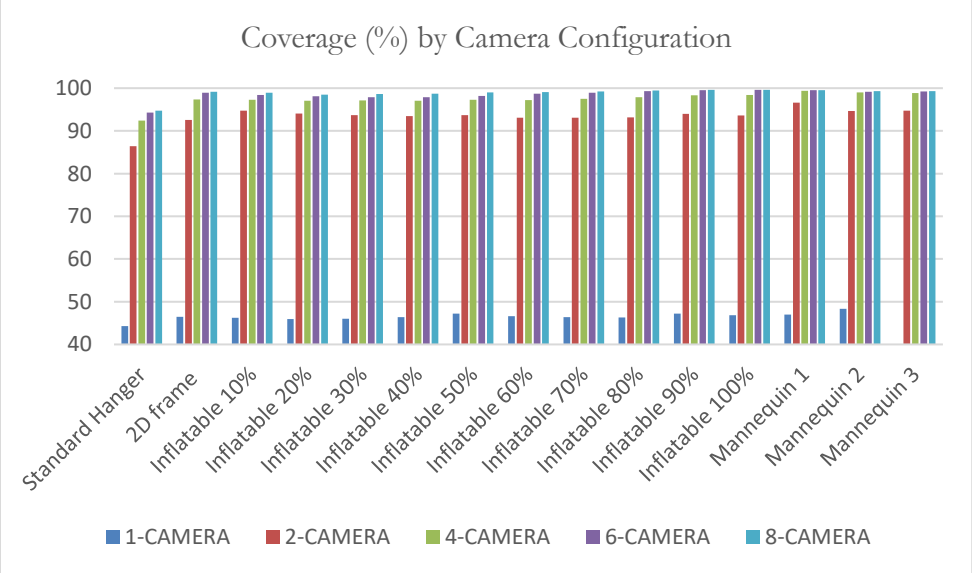

Figure 11 Coverage percentage by camara configuration

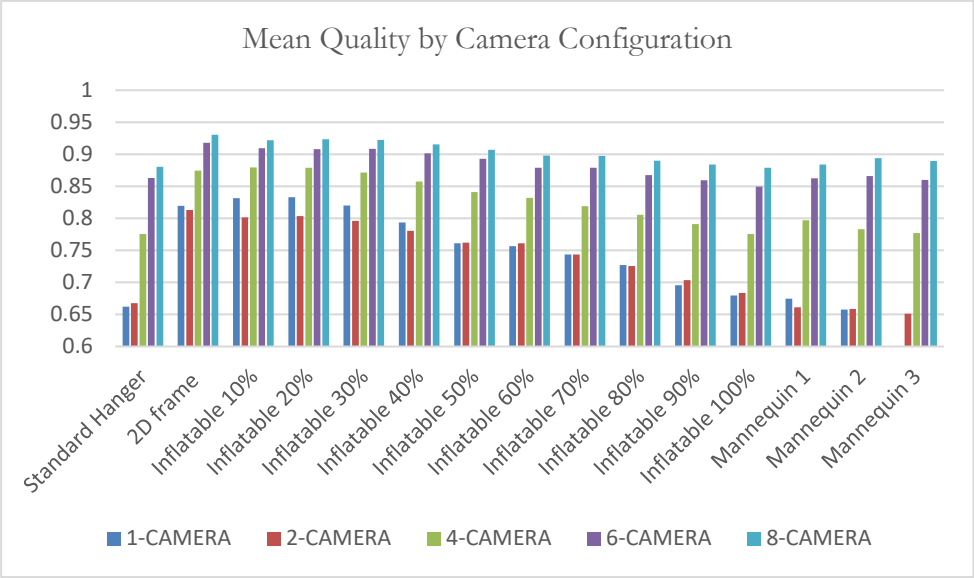

Figure 13 Mean Quality by Camera Configuration

The Efficiency Score shows in Figure 12 serves as a vital metric for Design for Automation (DfA), as it identifies the optimal balance between visual performance and system complexity. The analysis reveals that the 4-camera and 6-camera configurations yield the highest efficiency ratings, whereas the 8-camera setup shows diminished returns due to the high hardware overhead for negligible data improvement.

While the 2D frame exhibits high efficiency (85.13%) due to its simplicity, it lacks the 3D volume required to maintain the garment's natural shape. The baseline Standard Hanger consistently underperforms, showing the lowest efficiency scores across all configurations, which confirms that traditional hanger designs are inadequate for high-efficiency robotic handling and AI analysis.

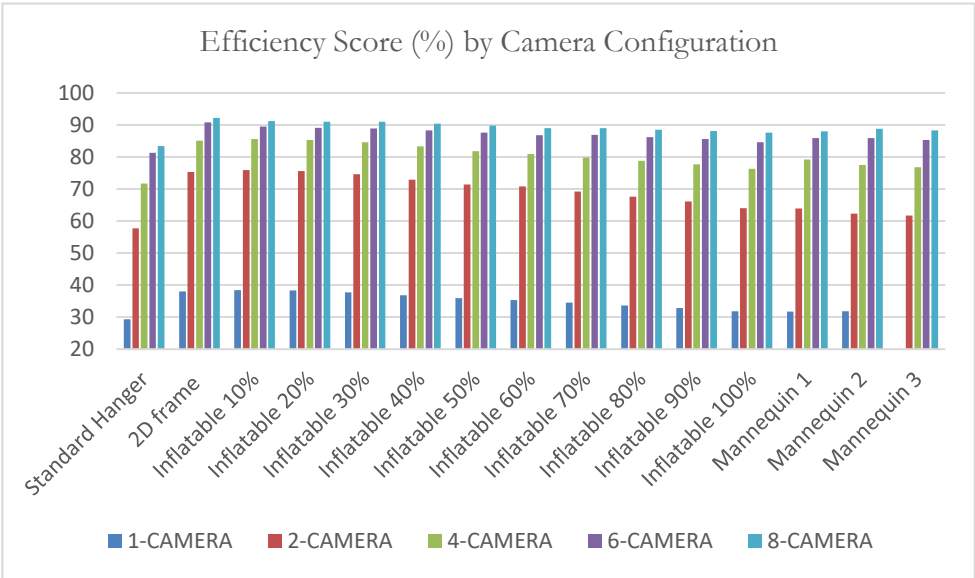

Figure 12 Efficiency Score (%) by Camera Configuration

4.7 Conclusion for the Next Phase of Development

Based on a comprehensive synthesis of the performance metrics, the next phase of development pivoted toward a hybrid geometry, modeled after the 2D frame and 20% inflatable configuration. While Mannequin 1 offers high raw coverage, the 2D frame and low-volume inflatable models demonstrate superior Efficiency Scores, reaching up to 85.13% and 85.32% respectively in a 4-camera setup, alongside significantly higher Mean Quality scores. By adopting a 20% inflatable 2D frame design, the project can maintain the streamlined, "slim" profile necessary for high-efficiency "blind" robotic insertion while providing enough volumetric depth to maintain the garment's natural shape for AI analysis.

The 4-camera configuration was standardized for the simulated prototype, as it represents the optimal balance of camera angles. This setup provides a coverage of approximately 97.06% for the 20% inflatable model, maximizing performance before encountering the diminishing returns of more complex 6- or 8-camera systems. Furthermore, the 4-camera configuration ensures high-fidelity data acquisition without the pixel dilution typically observed in larger volumetric models.

4.8 Validation of the Hybrid Geometry

The subsequent testing of the finalized Hybrid model that showed in the Figure 14confirms this strategic pivot. As shown in the updated performance data, the Hybrid geometry achieves a superior Efficiency Score of 89.06% in the 4-camera configuration [0, 63, 32, 6], surpassing both the 2D frame (85.13%) and the Inflatable 20% (85.32%) as shown in the Figure 15. Crucially, the Hybrid model also demonstrates the highest surface visibility across all tested configurations. It achieves a Coverage of 99.52% with only 4 cameras, which is essentially equivalent to its performance with 6 cameras (99.52%) and nearly matches the 8-camera maximum of 99.68% as shown in the Figure 16. Notably, the Hybrid geometry provides a remarkable 98.78% coverage with just 2 cameras, outperforming the 4-camera coverage of the 2D frame (97.37%) and the Inflatable 20% (97.06%).

These results, visualized in the simulated interaction in Figure 14, validate that the Hybrid geometry provides the most robust foundation for the next phase. Next phase was focused on refining this geometry to ensure that the increased efficiency and peak coverage directly translate into faster robotic handling cycles and more reliable AI surface inspections.

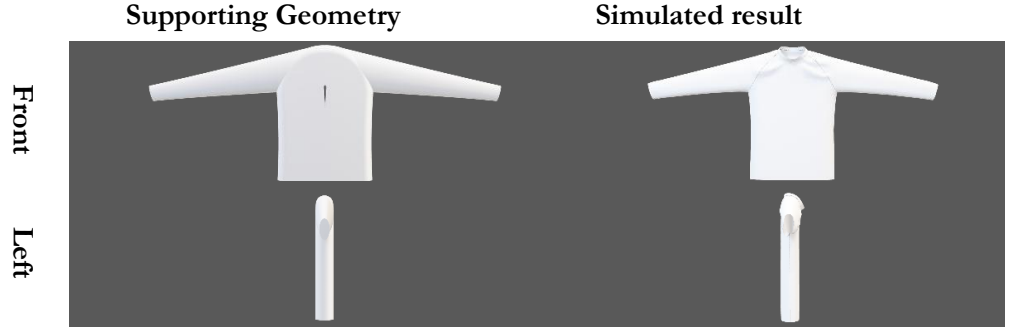

Figure 14 Hybrid geometry and the simulated garment

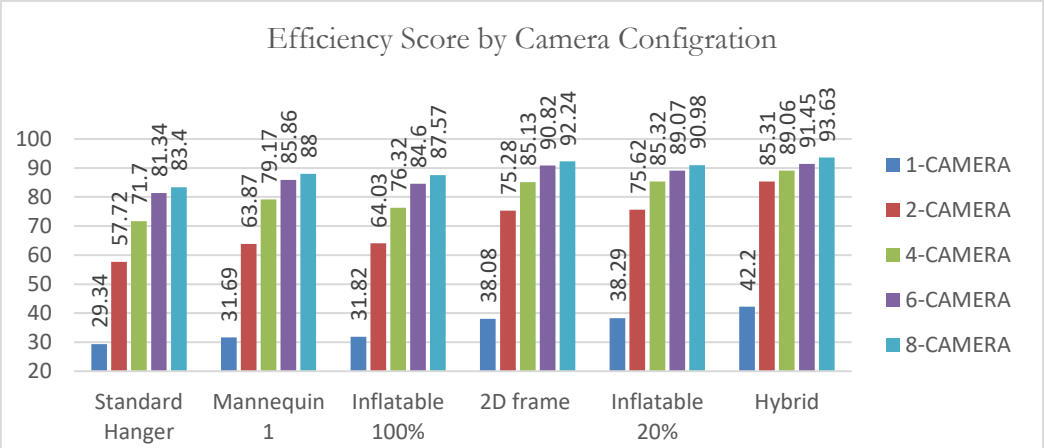

Figure 15 Efficiency score by camera configuration compression with hybrid geometry

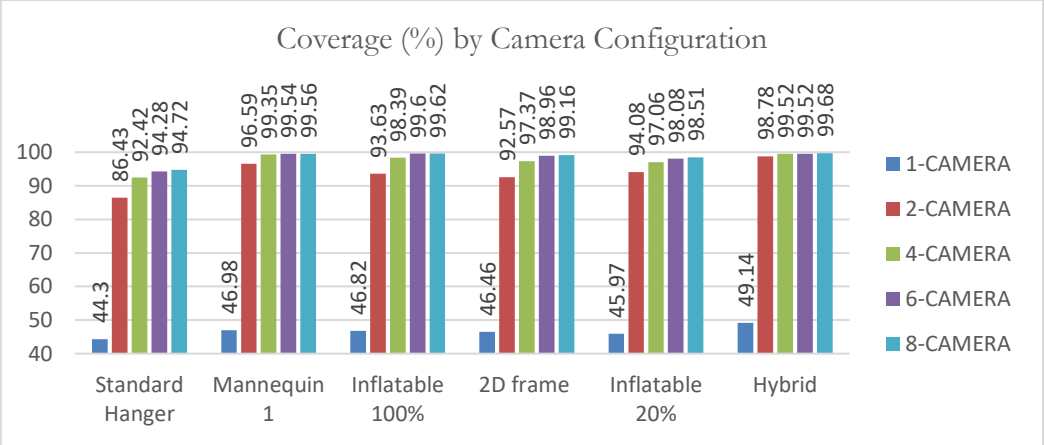

Figure 16 Coverage by camera configuration compression with hybrid geometry

4.9 Development of the Deployable Hanger Concept

The geometry evaluation showed that improved garment presentation requires greater separation between the front and rear garment surfaces. However, increasing the size of the supporting structure introduces a conflicting requirement for the automated hanging operation. A geometry that provides good support and surface exposure after hanging may be too large to pass reliably through the neckline of a garment. Therefore, the hanger could not be designed only for its final supporting condition. It also required a compact configuration during insertion. This requirement is consistent with the hybrid-design direction developed in the preceding geometry study, where a relatively thin structure was preferred to maintain compatibility with automated insertion.

To address these conflicting requirements, a deployable hanger concept was developed. The main design principle was to separate the hanger operation into two functional states: a compact insertion state and an expanded garment-support state. In the compact state, the dimensions of the hanger are reduced so that the mechanism can enter through the neckline with minimum interference. After insertion, the supporting elements are deployed to increase the effective width of the hanger and provide support across the shoulder region of the garment.

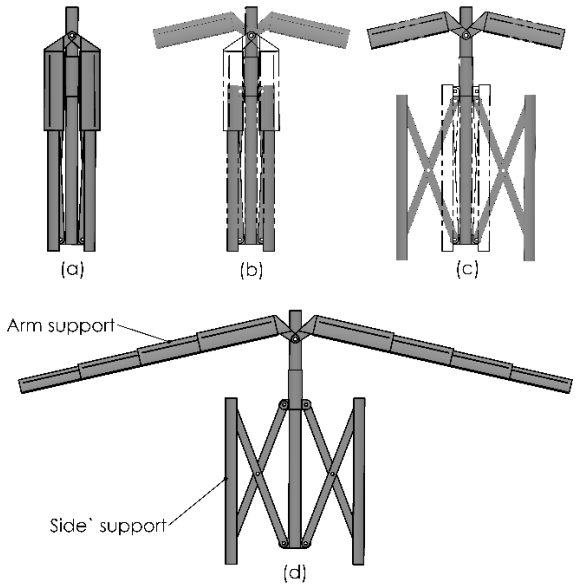

Figure 17 Operating principle of the deployable hanger concept: (a) compact configuration before insertion, (b) rotational deployment of the supporting arms, (c) extension of the side supports and (d) extension of the arm support

The developed concept consists of a central insertion section connected to two deployable supporting arms. During insertion, the arms remain in a folded configuration close to the central structure. Once sufficient insertion has been achieved, the left and right arms can rotate outward toward the garment shoulders. Telescopic sections are incorporated into the supporting arms so that the hanger width can be increased further after the initial rotational deployment. The combination of rotational and telescopic motion allows the mechanism to maintain a relatively small insertion envelope while still achieving a considerably larger supporting width after deployment.

This arrangement was selected instead of a fixed-width hanger because a fixed geometry would require the same dimensions to satisfy both insertion and garment-support requirements. These requirements are contradictory. Increasing the fixed hanger width improves shoulder support but reduces the available clearance during neckline insertion, while reducing the hanger width simplifies insertion but provides insufficient support after hanging. The deployable design therefore transfers part of this geometric conflict from the insertion trajectory to the mechanical structure itself.

The operating principle of the concept is illustrated in Figure X. Before insertion, the hanger remains in its compact configuration with the supporting arms folded inward. The compact insertion section is then moved vertically through the garment neckline. After the insertion stage has provided sufficient clearance, the supporting arms rotate outward. The telescopic sections can subsequently extend to increase the overall supporting width and establish the final hanger configuration.

An important consideration during concept development was the geometry of the leading insertion section. Although the deployable mechanism reduces the overall envelope of the hanger during insertion, the shape of the section entering the neckline still influences the ability of the system to tolerate uncertainty in garment position and orientation. For this reason, the insertion geometry was evaluated separately from the final supporting geometry. The subsequent insertion experiments investigated several candidate geometries

and quantified their tolerance to translational and angular variation before the most promising candidates were evaluated under garment-pickup variation.

This separation between insertion geometry and final support geometry represents an important feature of the proposed design. The geometry required to enter the garment does not need to be identical to the geometry required to support the garment after insertion. Instead, the system can use compact and tolerant geometry during the most constrained part of the operation and mechanically transform into a larger supporting structure afterward. This approach reduces the need to compromise the final garment-support geometry solely to satisfy the neckline-insertion requirement.

The concept was developed iteratively using mechanical design and physics-based simulation. Initial mechanism-level simulations were used to verify the motion of the rotational and telescopic elements before garment interaction was introduced. When interaction with the deformable garment was considered, additional constraints became apparent. A mechanism that could deploy freely without a garment could experience increased resistance or restricted motion when contacting the textile. Consequently, the mechanical arrangement and collision geometry were refined to reduce unnecessary interference between the deployable components and the garment.

The insertion experiments also showed that successful operation depended not only on the hanger geometry but on the configuration of the garment neckline before insertion. Variation in the initial garment pickup could alter the position and shape of the neckline sufficiently to reduce the reliability of purely passive insertion. This observation led to the later introduction of an active neckline-opening operation using two additional grippers. The purpose of these grippers was not to form part of the final hanger but to temporarily control garment presentation during the critical insertion stage.

The resulting system concept therefore combines three complementary mechanical functions: a compact insertion geometry for entering the garment, temporary control of the neckline during insertion, and a deployable hanger structure capable of increasing its dimensions after entry. This follows the Design for Automation principle of reducing process uncertainty through mechanical design rather than relying entirely on sensing and corrective robotic motion.

4.10 Blind-Insertion Simulation and Evaluation

Following the selection of the hybrid hanger geometry, a second simulation stage was conducted to evaluate whether the proposed design could support blind robotic insertion. The previous geometry evaluation considered the garment after it had reached a stable supported configuration. However, high surface exposure alone does not demonstrate that the geometry can be introduced into a deformable garment reliably. Therefore, a dynamic cloth-interaction experiment was developed to evaluate the insertion and deployment process.

4.10.1 Experimental Setup

The blind-insertion experiments were conducted in NVIDIA Isaac Sim using a deformable T-shirt model and a rigid insertion tool. To isolate the effects of insertion-tip geometry and initial pose uncertainty, the garment-picking condition and insertion motion were kept constant throughout all trials. Each experiment began from the same nominal garment presentation and reference tool pose. The garment was allowed to settle for 5.0 seconds before insertion, after which the tool moved 200 mm in the global vertical direction over 2.0 seconds. No continuous visual feedback, visual servoing, or corrective trajectory planning

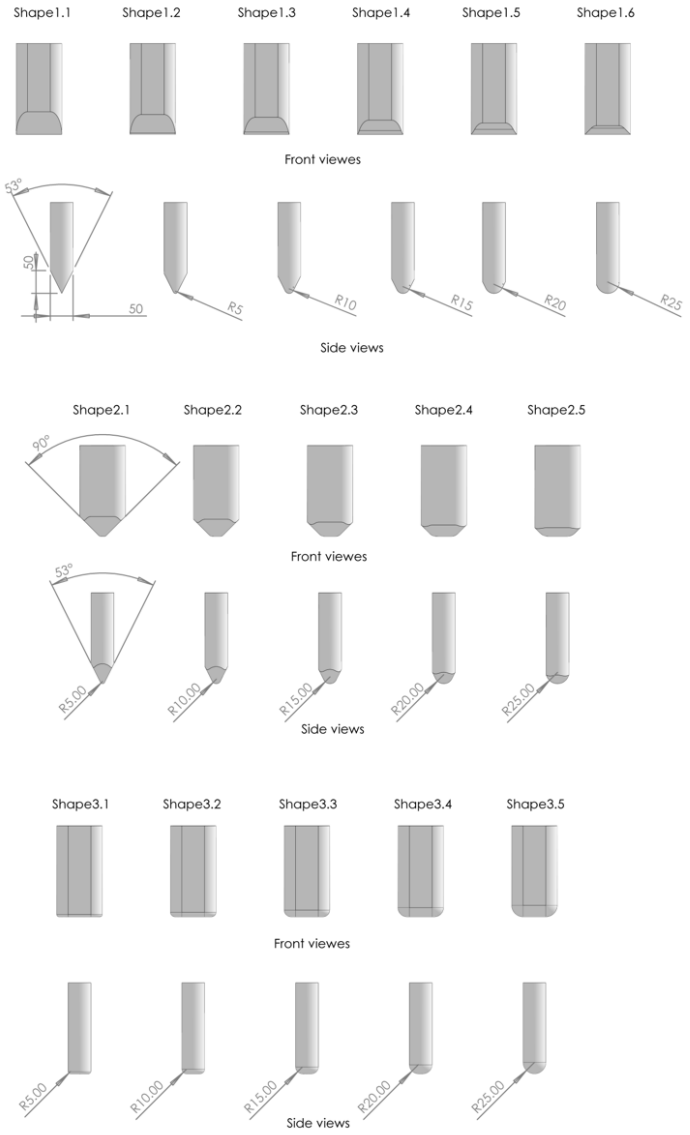

Figure 18 Evaluatted insertion-tip geometries

was applied once the insertion motion had started. A short final hold period was then used before evaluating the final geometric state.

Sixteen insertion-tip geometries as in the Figure 18 were mounted to the same rigid insertion-tool body so that the contacting geometry was the primary design variable, while the motion sequence remained unchanged. Controlled translational and rotational offsets were applied relative to the nominal pose to evaluate tolerance to initial alignment error. The evaluation was performed in stages so that the result of each stage guided the selection of candidates for the next experiment. First, all sixteen geometries were screened using Y-direction offsets from −20 mm to +20 mm in 1 mm increments, producing 656 trials.

Table 1 Results of the Y-offset screening for the 16 insertion-tip geometries. Ranking was based primarily on the width of the continuous successful Y-offset range, followed by the number of successful trials and the section-clearance margin.

Rank	Shape	Successful trials	Rate	Continuous successful Y range (mm)	Span (mm)
1	Shape2.5	17/41	41.46	-11 to +5	16
2	Shape2.3	14/41	34.15	-9 to +4	13
3	Shape3.1	13/41	31.71	-12 to 0	12
4	Shape3.2	13/41	31.71	-10 to +2	12
5	Shape3.3	14/41	34.15	-11 to 0	11
6	Shape1.3	12/41	29.27	-9 to +2	11
7	Shape1.5	12/41	29.27	-9 to +2	11
8	Shape2.2	12/41	29.27	-8 to +3	11
9	Shape2.4	15/41	36.59	-10 to 0	10
10	Shape1.6	11/41	26.83	-9 to +1	10
11	Shape1.2	11/41	26.83	-8 to +2	10
12	Shape1.4	11/41	26.83	-9 to +1	10
13	Shape1.1	10/41	24.39	-8 to +1	9
14	Shape2.1	12/41	29.27	-6 to +2	8
15	Shape3.4	10/41	24.39	-6 to +1	7
16	Shape3.5	0/41	0.00	None	0

The ranking in the Table 1 was based primarily on the continuous successful interval rather than the total number of isolated successful points. For example, Shape2.4 achieved 15 successful trials, which was more than Shape3.1 or Shape3.2, but its longest continuous window was only 10 mm. A broad continuous interval was considered more representative of useful mechanical tolerance for blind insertion. Shape2.5 produced the widest continuous successful Y-offset range, from −11 mm to +5 mm. Shape2.3, Shape3.1, and Shape3.2 also demonstrated comparatively wide continuous success regions. These four geometries were therefore selected for the subsequent X-offset screening.

The second screening stage demonstrated substantially greater tolerance in the X direction once each design was positioned near the center of its successful Y region. Shape2.3 succeeded in all 13 tested conditions from -30 mm to +30 mm. Shape2.5 succeeded in 12 of 13 trials, while Shape3.1 and Shape3.2 each succeeded in 11 of 13 trials. These results indicate that, for the tested garment presentation, Y alignment is more restrictive than X alignment. Summary of the second stage screening present in the Table 2.

Table 2 X-offset screening results for the four insertion-tip geometries selected from the Y-offset study. Each geometry was evaluated across X offsets from −30 mm to +30 mm at the Y position corresponding to the center of its continuous successful Y range.

Shape	Fixed Y (mm)	Success	Rate (%)	Continu-ous X suc-cess (mm)	Span (mm)
Shape2.3	-3	13/13	100.00	-30 to +30	60
Shape2.5	-3	12/13	92.31	-30 to +20	50
Shape3.1	-6	11/13	84.62	-25 to +25	50
Shape3.2	-4	11/13	84.62	-25 to +25	50

Shape2.3 was selected for the final angular study because it combined a useful Y tolerance with complete success across the full tested X range. At X = 0 mm and Y = -3 mm, all 11 X-axis rotation conditions from -15 deg to +15 deg were successful. Rota-tion about the Y axis was more restrictive: 7 of 11 trials succeeded, corresponding to a continuous successful range from -9 deg to +9 deg. The directional difference con-firms that pose uncertainty is anisotropic and that the insertion geometry is more tolerant to some orientation errors than others.

Figure 19 illustrates the garment position after the 5 second settling period, together with the initial insertion-tool location and the gripper arrangement used during Stage 1, Stage 2, and the angular-error evaluation.

4.10.2 Evaluation of Garment-Pickup Variation

One of the main practical uncertainties in the proposed blind-insertion system is the repeatability of the garment-picking operation. Even if the insertion tool follows the same trajectory, variations in the locations at which the garment is grasped can change the position, orientation, and shape of the neckline after the garment is lifted. Therefore, an additional simulation study was conducted to evaluate how sensitive the insertion process was to changes in garment pickup location. The objective of this experiment was not to introduce an error directly to the insertion tool, as in the previous translational and angular-error studies, but instead to determine whether the selected insertion geometries could accommodate changes in garment presentation resulting from pickup uncertainty.

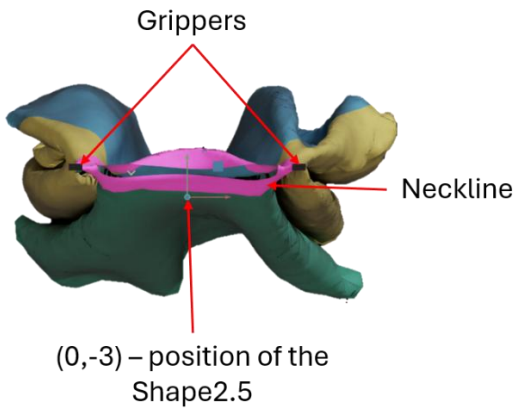

Figure 19 Stage 2 simulation state after a 5 second garment-settling period prior to insertion.

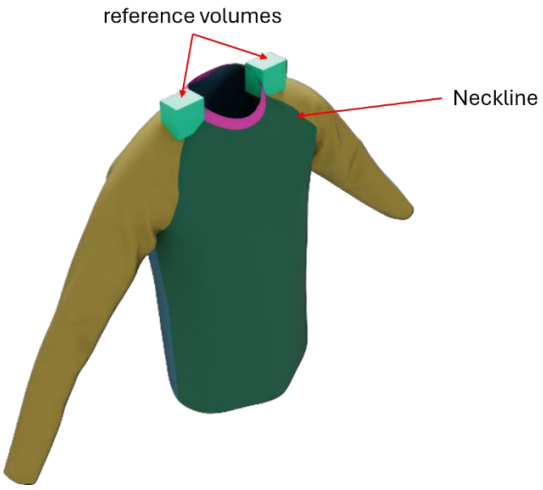

Figure 20 Reference volumes used to define the allowable left and right garment-pickup regions for the pickup-variation analysis.

As in the Figure 20, two reference volumes were defined over the allowable left and right pickup regions of the T-shirt. Before each simulation was started, garment vertices located inside these reference volumes were identified and used to generate alternative grasp locations. A sampling distance of approximately 10 mm, corresponding to the size of the gripper contact region, was used to avoid testing nearly identical pickup positions. This procedure identified 31 possible pickup locations on the left side and 38 on the right side. Testing every possible left-right combination would have resulted in 1,178 pickup configurations; therefore, nine representative left-right combinations were selected to cover different regions and directions of pickup displacement.

For each trial, the simulation was first stopped, and the selected garment vertices were assigned to the left and right gripper attachments. The grippers were then repositioned to the corresponding new pickup locations while maintaining their original orientations. This ensured that the garment was already attached at the new pickup locations before the physics simulation began. After the new grasp configuration had been established, the insertion-tool starting position was translated according to the displacement of the midpoint between the two grippers. This maintained the relative relationship between the garment and insertion tool established during the previous experiments, while retaining the selected Y-direction insertion bias of −3 mm.

After the pickup configuration had been established, the simulation was started and the garment was allowed to settle under deformable-body physics for 5 seconds. The insertion tool was then moved 200 mm in the vertical direction over 2 seconds using the same blind-insertion trajectory and final-state evaluation criteria applied in the previous tests. No visual feedback or corrective trajectory planning was applied during the insertion. Two of the previously selected insertion geometries, Shape2.3 and Shape2.5, were evaluated for each of the nine pickup configurations.

The first trial for each pickup configuration was performed with no additional X-direction correction to the insertion-tool position. This condition was used to evaluate the passive tolerance of the insertion geometry to pick up variation. When an insertion failed at this nominal condition, additional recovery trials were performed by shifting the insertion tool along the X direction in 5 mm increments within a range of −40 mm to +40 mm. The correction magnitude was increased progressively until a successful insertion was obtained or the complete correction range had been evaluated. This second part of the test was intended

to determine whether failures caused by pickup variation could be compensated for using a simple adjustment of the insertion-tool starting position.

4.10.3 Pickup-Variation Results

The results in Table 3 showed that changes in garment pickup location had a noticeable effect on the blind-insertion process. Without any additional X-direction correction, Shape2.3 successfully completed insertion for 5 of the 9 pickup configurations, corresponding to a direct success rate of 55.56%. Shape2.5 successfully completed 6 of the 9 configurations, corresponding to a direct success rate of 66.67%. Shape2.5 therefore demonstrated greater passive tolerance to variation in the initial garment pickup condition.

Table 3 Summary of direct and recovered insertion performance for Shape12 and Shape14 under varied garment-pickup configurations.

Geometry	Direct success (X = 0)	Direct success rate	Recovered configurations	Final successful configurations	Final success rate
Shape2.3	5/9	55.56%	3	8/9	88.89%
Shape2.5	6/9	55.56%	1	7/9	77.78%

The recovery tests demonstrated that several of the failed pickup conditions could still be accommodated by adjusting the X position of the insertion tool. For Shape2.3, three of the four initially unsuccessful configurations were recovered. Successful corrections of +5 mm, −30 mm, and −40 mm were identified for different pickup configurations. This increased the successful coverage of Shape2.3 from 5/9 to 8/9 configurations (88.89%). For Shape2.5, one of the three failed configurations was recovered using an X correction of −25 mm, increasing its successful coverage from 6/9 to 7/9 configurations (77.78%).

Considering both geometries, 11 of the 18 geometry–pickup combinations succeeded without additional correction. After the X-direction recovery procedure was applied, 15 of the 18 combinations could be successfully inserted, corresponding to an overall successful coverage of 83.33%.

The results also showed a difference between the two insertion geometries. Shape2.5 provided the higher direct success rate and therefore showed better passive tolerance to pick up uncertainty. In contrast, Shape2.3 showed greater recoverability when the insertion-tool position was adjusted, with only one of its nine pickup configurations remaining unsuccessful after the recovery search. This indicates that the preferred geometry may depend on whether the final automation concept is intended to rely entirely on passive mechanical tolerance or whether a simple positional correction of the insertion tool is available.

Most unsuccessful trials were associated with the neckline no longer surrounding the insertion-tool axis or with only partial entry of the insertion geometry. This indicates that the main effect of pickup-location variation was a change in the resulting neckline position and configuration rather than direct penetration of the garment by the tool. In other words, changing the pickup points can cause the neckline to relax into a position where the available opening is no longer correctly aligned with the blind-insertion trajectory.

4.10.4 Active Mechanical Control of the Neckline Opening

Following the pickup-variation study, the remaining insertion failures were found to be associated primarily with changes in the position and configuration of the neckline. Although adjustment of the insertion-tool position recovered several failed conditions, positional correction alone could not compensate for all changes in garment presentation. Therefore, an

additional mechanical operation was introduced to actively enlarge and stabilize the neckline before insertion.

Two additional grippers were positioned on opposite sides of the garment, corresponding to the front and rear surfaces of the neckline region. Unlike the initial garment-pickup grippers, no predefined garment location was assigned for these grippers to grasp. Instead, both grippers were positioned at the same height and X-coordinate and approached the garment from opposite directions. After the garment had settled for 5 seconds, the grippers moved toward the garment until contact was established with the front and rear garment surfaces.

Once contact had been established, the grippers held the contacted garment regions and moved outward in opposite directions. Each gripper was displaced by 30 mm, producing a total increase of approximately 60 mm in the separation between the front and rear garment surfaces. This operation mechanically enlarged the available opening before the insertion tool entered the garment.

After the neckline had been opened, the insertion tool followed the same 200 mm vertical insertion trajectory over 2 seconds used in the previous experiments. The opening grippers maintained the garment separation during the initial part of the insertion. After approximately 140 mm of insertion, the temporary grip was released so that the garment could move freely around the insertion geometry during the remaining motion.

The same nine representative pickup configurations previously evaluated were tested using Shape2.3 and Shape2.5. No additional X-direction correction was applied during these trials. This allowed the performance of active neckline opening to be directly compared with the passive insertion results obtained under the same pickup-variation conditions.

4.10.5 Active-Opening Result

The active neckline-opening operation substantially improved robustness to garment-pickup variation. Shape2.3 successfully completed insertion for all nine representative pickup configurations, increasing its direct successful coverage from 5/9 (55.56%) without active opening to 9/9 (100%). Shape2.5 similarly increased from 6/9 (66.67%) to 9/9 (100%).

Table 4 Effect of active neckline opening on pickup-variation robustness

Geometry	Passive direct insertion (X = 0)	After X-recovery	Active neckline opening
Shape2.3	5/9 (55.56%)	8/9 (88.89%)	9/9 (100%)
Shape2.5	6/9 (66.67%)	7/9 (77.78%)	9/9 (100%)

Considering both geometries, the passive blind-insertion configuration successfully completed 11 of the 18 geometry–pickup combinations without positional correction. With active mechanical control of the neckline, all 18 geometry–pickup combinations completed successfully, corresponding to an overall success rate of 100%. This represents an increase of 38.89 percentage points relative to the passive direct-insertion condition.

The active-opening configuration also exceeded the performance obtained using X-direction recovery. Positional recovery increased the successful coverage of the previous experiment to 15/18 (83.33%), whereas active neckline opening achieved 18/18 successful insertions without requiring individual X-direction corrections. In Figure 21, the top row shows the passive insertion sequence, where the neckline remains narrow and the insertion geometry is not reliably guided through the garment. The bottom row shows the active-opening sequence, where the front and rear garment surfaces are mechanically separated

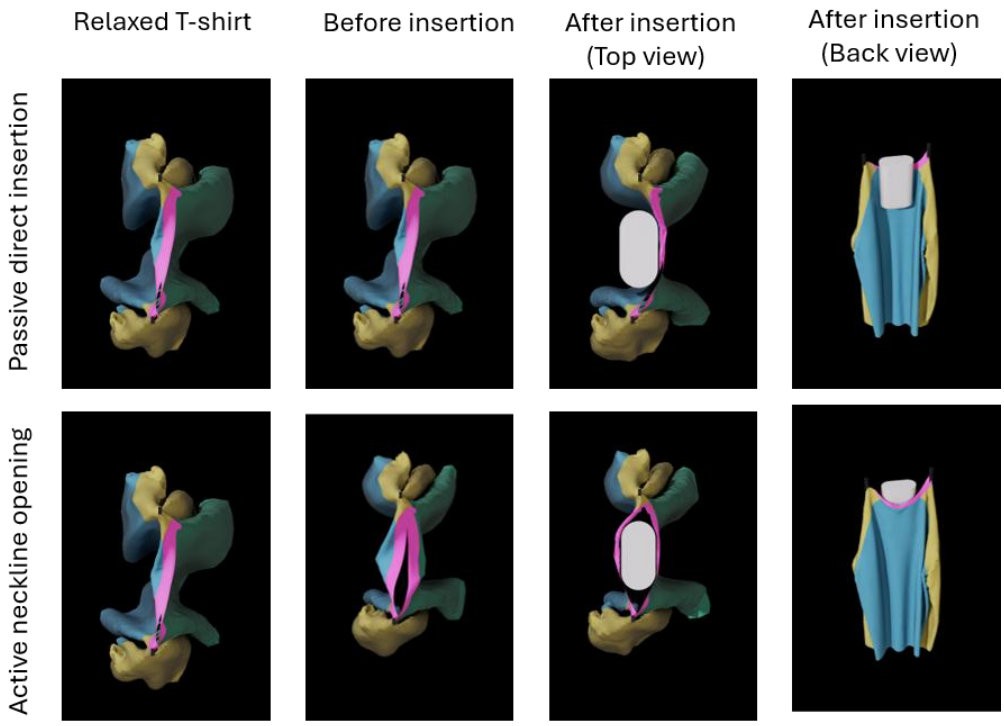

Figure 21 Comparison of blind insertion without and with active neckline opening under the same garment-pickup condition.

before insertion, creating a wider and more stable neckline opening and enabling successful insertion.

All Stage 4 trials completed the full 200 mm insertion and satisfied the existing geometric success criteria. The neckline surrounded the insertion-tool axis, a valid tool cross-section was detected within the neckline, and no final garment-body penetration was detected in any of the 18 trials. This indicates that mechanically controlling the neckline configuration reduced the sensitivity of blind insertion to variations introduced by the garment-picking operation.

4.10.6 Full Hanger-Cycle Simulation

The purpose of the full-cycle simulation was to determine whether the compact hanger could first enter the garment and subsequently expand into the larger geometry required for garment support and presentation. This directly addressed the earlier limitation that successful surface exposure does not necessarily imply successful garment automation.

The complete simulated sequence consisted of the following stages as shown in the Figure 22 and Figure 23:

1. The T-shirt was initially suspended using the left and right garment pickup grippers.
2. Temporary front and back grippers approached the garment and separated the front and back layers to increase the available opening around the neckline.
3. The compact hanger was inserted through the neckline.
4. The two main hanger arms were deployed to an intermediate angle of 60°.
5. The second telescopic arm sections were extended.
6. The third telescopic sections were extended.
7. The fourth telescopic sections were extended.

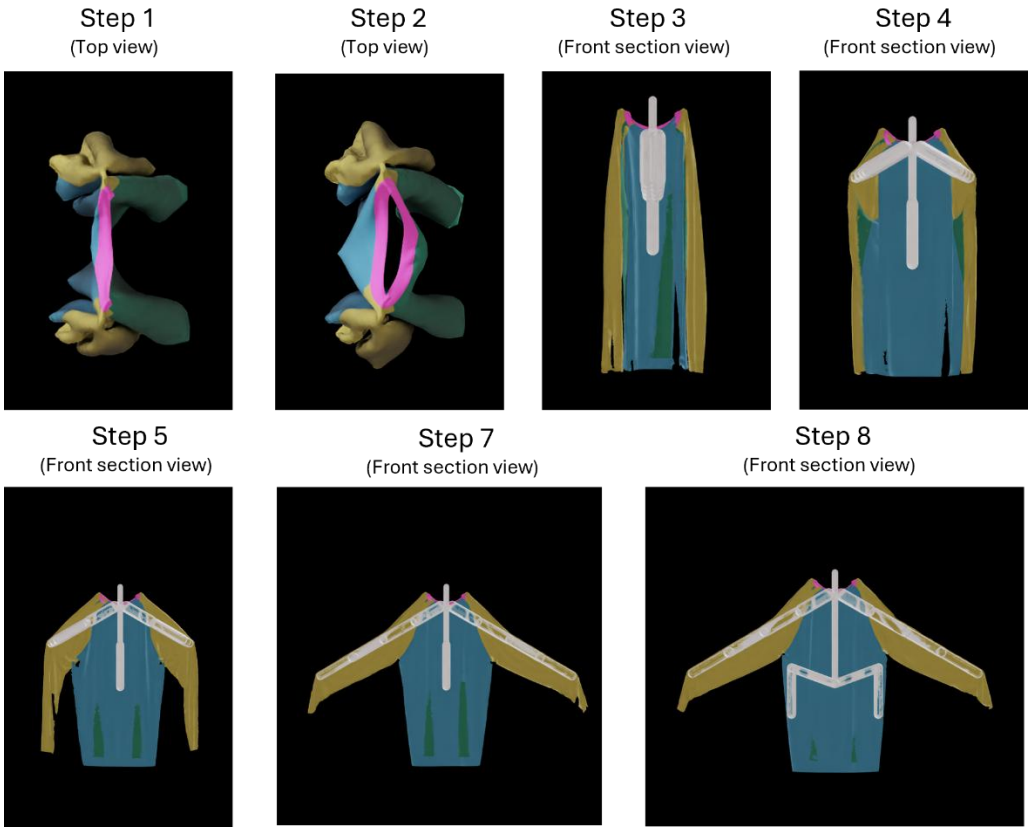

Figure 22 Sequential stages of the simulated full hanger cycle up to Stage 8, showing garment opening, compact hanger insertion, initial shoulder deployment, telescopic extension, and side-support deployment. The final shoulder expansion from 60° to 75°.

8. The side-support mechanisms were deployed.
9. The main hanger arms were finally rotated through the remaining 15°, resulting in a final shoulder deployment angle of 75°.
10. The left and right garment pickup grippers were released, and the garment was allowed to settle on the expanded hanger.

The simulation demonstrated that the individual mechanical operations developed during the study could be combined into a complete hanger-insertion and deployment sequence. This is an important result because the selected hanger concept intentionally separates two conflicting requirements: compact geometry is required during insertion, whereas a larger three-dimensional structure is preferred after insertion to improve garment presentation.

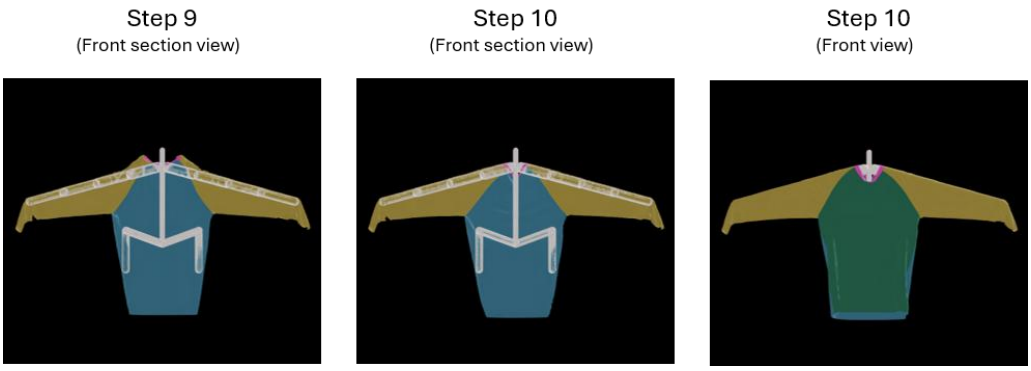

Figure 23 Final stages of the full hanger-cycle simulation, showing completion of the deployment sequence and the resulting supported garment configuration after the final shoulder expansion to 75°.

4.10.7 Modified shoulder-deployment sequence

During development of the complete cycle, the original deployment sequence had to be modified. Initially, the main hanger arms were commanded directly to their final 75° deployment angle before the telescopic sections had completed their motion as shown in the Figure 24. In the deformable simulation, this sometimes caused the shoulder sections of the hanger to penetrate through the T-shirt instead of pushing and redistributing the textile around the mechanism.

To reduce this numerical penetration, shoulder deployment was divided into two stages. The main arms were first deployed to 60°. The telescopic and side-support mechanisms were then allowed to complete their movements while the main arms remained at this intermediate position. Only after these stages had completed were the arms rotated through the remaining 15° to the final 75° position.

This modification should primarily be regarded as a simulation-specific deployment strategy rather than a strict requirement for the physical mechanism. In a physical system, hanger insertion and expansion could potentially occur simultaneously. For example, the shoulder arms could gradually open while the hanger is still moving through the neckline, and the telescopic sections could begin extending before the insertion axis has reached its final position. Such coordinated movement would allow the garment to slide continuously over the expanding structure and could reduce the total cycle time.

4.10.8 Evaluation of different size of garments

To evaluate whether the selected hanger dimensions and deployment sequence were applicable beyond the T-shirt used during the main development experiments, additional trials were conducted using different upper-body garment models. The garments were selected from the USD assets available in the Garment Lab collection under Garment/Tops/Collar_Lsleeve_FrontClose/[23]. The same hanger dimensions and general deployment sequence developed during the previous experiments were retained so that the effect of garment size and geometry could be evaluated without modifying the mechanism for each individual garment.

The trials showed that the developed hanger configuration produced viable results for the tested male upper-body garments approximately within EU sizes 48–54. Within this range, the compact hanger could be introduced through the neckline and subsequently expanded using the developed shoulder and telescopic deployment sequence. The garments were able to redistribute around the expanding hanger and reach a supported final configuration without requiring a separate hanger with different dimensions.

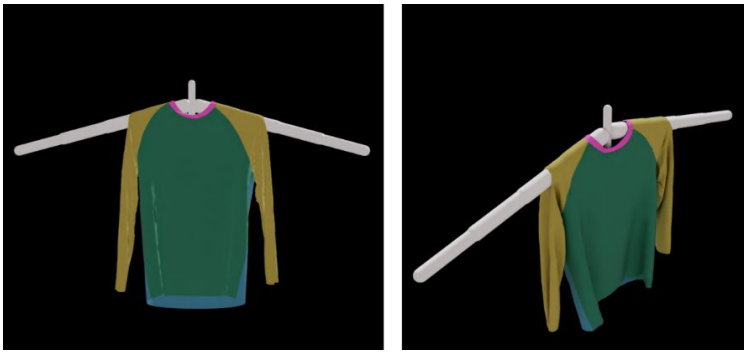

Figure 24 Final stages of full hanger-cycle simulation without intermediate 60° shoulder expansion.

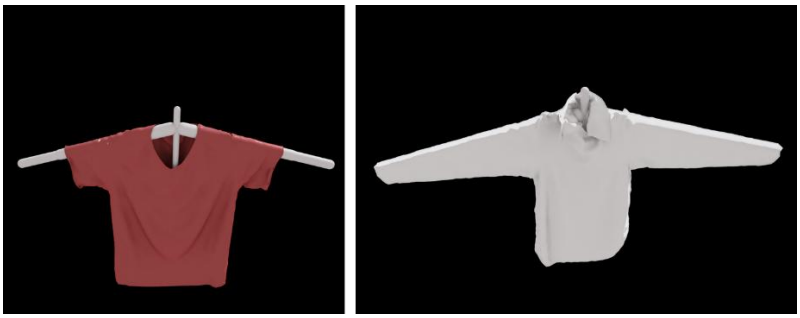

Figure 25 Sample of garments from GarmentLab assets that success with the deployment.

These results suggest that the selected mechanism dimensions provide a useful operating range rather than being limited to one specific garment. In particular, the telescopic sections allow the supporting width of the hanger to increase after insertion, making the final geometry adaptable to variation between garment sizes while maintaining the same compact insertion configuration.

However, the trials also identified clear limits to this operating range. Smaller garments experienced greater difficulty during shoulder deployment. As the shoulder arms opened and the telescopic sections expanded, the available internal space of the garment became insufficient for the selected deployment dimensions. This increased the interaction between the hanger and the garment and could prevent the textile from sliding correctly over the expanding structure.

The problem was particularly noticeable for female garment geometries with a relatively narrow under bust region. Although the hanger could enter the garment, the expansion required to achieve the selected final support geometry could exceed the available internal garment width. In these cases, the final hanger configuration was therefore too large relative to the garment geometry.

A second limitation was identified at the neckline. Garments with a narrow neckline, particularly those with a neckline circumference below approximately 120 mm in the evaluated assets, could not provide sufficient clearance for reliable insertion of the compact hanger geometry. These garments therefore failed before the deployment stage because the initial insertion envelope of the hanger remained too large relative to the available opening.

The different-garment trials therefore indicate that two separate geometric constraints determine whether the developed hanger can be used successfully:

> Neckline clearance during insertion, which determines whether the compact hanger can enter the garment.
> Available garment width during deployment, which determines whether the shoulder and telescopic mechanisms can expand without excessive interference with the textile.

The selected hanger dimensions consequently represent a practical operating range rather than a universally compatible geometry. Within the tested simulations, the configuration was suitable for male upper-body garments approximately within EU sizes 48–54, while smaller garments and garments with narrow neckline or under bust geometries were more likely to fail.

This result also highlights an important requirement for future development. To increase compatibility across a broader garment population, the final mechanism may require size-dependent deployment rather than always expanding to the same fixed dimensions. For example, the shoulder angle or telescopic extension could be limited according to an estimated

garment size, allowing the hanger to provide sufficient support without forcing a small garment toward the maximum deployment configuration.

The additional garment trials therefore provide preliminary evidence that the developed deployable-hanger concept can generalize across multiple upper-body garment sizes, while also identifying the neckline opening and internal garment width as important geometric boundaries for successful operation.

5 Results and discussion

The experimental evaluation was conducted in two main stages. First, a range of garment-support geometries was compared to determine how the supporting structure influences garment surface visibility and observation quality. Second, the results of this comparison were used to develop and evaluate a hybrid hanger geometry intended to combine the favorable visual characteristics of volumetric support with the compact profile required for subsequent automated insertion.

5.1 Influence of Supporting Geometry on Surface Exposure

The initial evaluation included a standard hanger, a two-dimensional frame, three mannequin configurations, and a series of inflatable geometries with different degrees of volumetric expansion. The objective was to determine how progressively increasing the depth of the supporting geometry affected the visibility and observation quality of the garment surface.

The results demonstrate that geometry supporting the garment has a significant effect on surface exposure. The standard hanger consistently produced the lowest performance among the evaluated geometries. This can be attributed to the relatively flat hanging configuration, which allows the front and rear layers of the garment to remain close to each other and creates folds and occluded regions.

In contrast, the mannequin and inflatable configurations increased the three-dimensional separation of the garment surfaces. As a result, surface visibility increased considerably. With four cameras, most of the volumetric geometries achieved above 97%, with Mannequin 1 reaching approximately 99.35%.

This result demonstrates that increasing the spatial separation between garment surfaces can substantially reduce self-occlusion. However, maximizing coverage alone was not sufficient for determining the optimal geometry.

5.2 Observation Quality and the Influence of Geometry

The Mean Sampling Integrity results show a different trend from the surface-coverage results. Although highly volumetric geometries achieve high visibility, observation quality decreases as the garment surface becomes increasingly curved relative to the available camera viewpoints.

The two-dimensional frame achieved a Mean Sampling Integrity of approximately 0.8743 using four cameras, representing one of the highest values among the evaluated configurations. Its thin geometry exposes a large proportion of the garment while limiting highly oblique viewing angles.

This creates an important design trade-off. A purely planar geometry provides high observation quality but does not reproduce the natural three-dimensional form of a worn garment. Conversely, a highly volumetric geometry improves surface separation and total visibility but creates surfaces that are observed at increasingly oblique angles.

The results therefore indicate that neither the standard hanger nor a full mannequin-like geometry represents the optimal solution for the intended automated system. Instead, intermediate geometry is desirable.

5.3 Influence of the Number of Cameras

A second important result concerns the number of cameras required to observe the garment effectively.

The largest improvement in surface coverage occurred between the single-camera and two-camera configurations. Additional cameras continued to improve coverage, although the magnitude of improvement decreased considerably as the number of cameras increased.

For many of the evaluated geometries, four cameras already provided surface coverage greater than 97%. Increasing the number of cameras from four to six or eight produced comparatively small improvements in visibility.

Consequently, the four-camera configuration was selected as the reference arrangement for further concept development. This selection does not imply that four cameras provide the absolute mathematical maximum observation quality. Rather, four cameras represent a practical compromise in which a high level of surface visibility and sampling quality is achieved before the additional improvement obtained from further viewpoints becomes relatively small.

This distinction is important because the observation-quality metric itself does not include hardware cost or system complexity. Therefore, the selection of four cameras is an engineering trade-off based on diminishing improvement rather than completely depending on the numerical maximum of the calculated metric.

5.4 Saliency-Weighted Evaluation

The initial evaluation treated all garment surface regions with equal importance. However, this does not fully represent the requirements of garment inspection, since some regions may contain more relevant information for defect detection or garment-quality assessment than others.

A saliency-weight reference map was therefore introduced. The weighted calculation increased the importance of selected garment regions, particularly areas around the chest, shoulders, seams, and other zones considered important for garment inspection.

The use of the saliency map changes the camera-selection objective from maximizing total geometric visibility to maximizing the quality of information obtained from the most relevant surface regions.

This approach provides a closer link between hanger geometry and the intended downstream application. Nevertheless, the weighting remains an engineering approximation of the relative importance of garment regions.

5.5 Selection of the Hybrid Geometry

Evaluation of the initial geometries identified the two-dimensional frame and the low-volume inflatable configurations as promising candidates.

Using four cameras, the two-dimensional frame achieved an Efficiency Score of approximately 85.13%, while the 20% inflatable geometry achieved approximately 85.32%. These configurations provided a favorable combination of surface coverage and observation quality while maintaining considerably less depth than a mannequin.

Based on these results, a hybrid geometry was developed. The design combines the overall planar structure of the two-dimensional frame with a limited amount of three-dimensional depth inspired by the low-volume inflatable concept.

The intention was to preserve the thin profile required for subsequent automated insertion while providing sufficient spatial separation to reduce folds and occlusion.

5.6 Validation of the Hybrid Geometry

The hybrid geometry produced the strongest overall performance of the final evaluated configurations.

With four cameras, the hybrid geometry achieved a surface coverage of 99.52% and an Efficiency Score of 89.06%. This exceeds the corresponding four-camera Efficiency Scores of the two-dimensional frame (85.13%) and the 20% inflatable geometry (85.32%).

The high surface coverage was also maintained when the number of cameras was reduced. With only two cameras, the hybrid geometry achieved 98.78% surface coverage. This is greater than the four-camera coverage of both the two-dimensional frame, at 97.37%, and the 20% inflatable configuration, at 97.06%.

Increasing the hybrid configuration from four cameras to six cameras produced essentially no improvement in coverage, with both configurations giving approximately 99.52%. Eight cameras increased coverage only slightly to approximately 99.68%.

These results indicate that hybrid geometry provides a strong compromise between compactness, garment surface separation, visibility, and angular observation quality.

5.7 Full Hanger-Cycle Simulation

The full hanger-cycle simulation integrated the individual developments of the previous experiments into a complete hanging sequence. The purpose of this stage was to determine whether the garment could be maintained in a suitable configuration for insertion, whether the compact hanger could pass through the neckline, and whether the same mechanism could subsequently transform into the larger supporting geometry required for garment presentation. This integration was particularly important because the geometry preferred for final garment support is fundamentally different from the geometry preferred during insertion. A large three-dimensional supporting structure improves garment presentation, whereas compact geometry is required to pass reliably through the neckline.

The full-cycle design therefore combined three functions developed during the earlier experiments: active mechanical control of the neckline, a compact insertion geometry, and a deployable supporting structure.

5.7.1 Active neckline control and insertion geometry

The front and back grippers were introduced as a direct result of the garment-pickup variation experiments. The initial left and right pickup grippers were sufficient to suspend the garment, but they did not directly control the separation between the front and rear garment surfaces. Consequently, changes in the pickup locations produced changes in the position and shape of the neckline. In several configurations, the neckline relaxed or collapsed sufficiently that the insertion-tool axis was no longer surrounded by the opening, even though the insertion trajectory itself remained unchanged.

The passive insertion results demonstrated the importance of this effect. Across Shape2.3 and Shape2.5, only 11 of the 18 tested geometry–pickup combinations completed the inser-

tion without additional positional correction. Introducing an X-direction correction increased this to 15 of 18 combinations. However, this required a different correction for different garment configurations and therefore reduced the suitability of the process for a blind and repeatable industrial operation.

The additional front and back grippers were introduced to control the garment configuration mechanically instead of compensating for each variation by modifying the hanger trajectory. The two temporary grippers approached the garment from opposite sides and contacted the front and rear surfaces close to the neckline. After establishing the temporary grasp, each gripper moved approximately 30 mm outward, producing approximately 60 mm of additional front-to-back separation. The objective was not to position the neckline into an exact predefined shape, but to create a sufficiently large and stable opening for the compact hanger to enter without simultaneously interacting with both garment layers.

This modification produced a substantial improvement in insertion robustness. With active neckline opening, both Shape2.3 and Shape2.5 successfully completed all nine pickup configurations, resulting in 18 successful geometry–pickup combinations out of 18 tested. This corresponds to an improvement from 61.11% successful coverage for passive direct insertion to 100% with active opening. More importantly, the result was obtained without individual X-direction corrections for different pickup conditions. Therefore, the front and back grippers can be considered an effective addition to the system because they reduced the sensitivity of the insertion process to variation introduced during the preceding garment-pickup operation.

The result also demonstrates an important Design for Automation principle of the proposed system. Instead of attempting to estimate the complete deformable neckline geometry and continuously correct the hanger trajectory, a relatively simple mechanical action was used to establish a more predictable state before insertion. The temporary opening grippers were therefore not part of the final garment-support system; their function was limited to reducing uncertainty during the most constrained stage of the hanging operation. Once approximately 140 mm of the 200 mm insertion motion had been completed, the temporary attachments could be released because the hanger had entered sufficiently far into the garment to continue guiding the textile.

The geometry of the hanger used during this stage was also the result of the earlier design-selection process. Two different geometric requirements had to be considered. The first was the geometry required for final garment presentation. The surface-exposure study showed that the hybrid geometry provided the strongest compromise between a thin profile and three-dimensional garment separation, achieving 99.52% surface coverage and an Efficiency Score of 89.06% using four cameras. This geometry was therefore preferred for the final expanded supporting condition.

The second requirement concerned the geometry that passes through the neckline. The insertion-tip experiments demonstrated that this geometry should be evaluated separately from the final supporting geometry. Shape2.5 provided the widest continuous successful Y-offset interval, from −11 mm to +5 mm, while Shape2.3 demonstrated complete success across the tested X-offset range from −30 mm to +30 mm. Shape2.3 also successfully tolerated all tested rotations from −15° to +15° about the X axis and a continuous range of approximately −9° to +9° about the Y axis. These results showed that a compact insertion geometry could provide useful mechanical tolerance to translational and rotational errors before the larger supporting structure was deployed.

The active-opening experiments further showed that hanger-tip geometry and garment preparation should not be considered independently. Shape2.3 and Shape2.5 exhibited different levels of passive tolerance during the pickup-variation study, but both achieved 100%

success after active neckline opening was introduced. This suggests that mechanically conditioning the neckline can reduce the dependence of insertion success on small differences between otherwise suitable insertion geometries. The final system concept therefore does not rely on hanger geometry alone; robustness is obtained through the combination of a tolerant insertion geometry and temporary mechanical control of the garment.

After the neckline had been opened, the hanger was moved through the neckline in its compact configuration. Only after sufficient insertion had been achieved was the mechanism expanded toward its final supporting geometry.

5.7.2 Staged deployment of the hanger

The deployment sequence also required modification during development of the full-cycle simulation. The intended final shoulder angle of the main hanger arms was 75°. Initially, the two main arms were commanded directly from their compact position to the full 75° angle before completion of the telescopic deployment. Although the rigid mechanism could perform this motion, its interaction with the deformable garment produced an undesirable result. In some simulations, the shoulder sections moved through the T-shirt mesh instead of gradually pushing and redistributing the fabric around the expanding hanger.

For this reason, the 75° shoulder deployment was divided into two stages. The main hanger arms were first rotated to an intermediate angle of 60°. At this position, the hanger already provided substantial lateral opening toward the shoulder regions while avoiding the more aggressive final expansion that had produced penetration in the direct 75° deployment.

While the main arms remained at 60°, the telescopic sections were extended sequentially, and the side-support mechanisms were deployed. Maintaining the shoulder arms at the intermediate angle provided additional space for these components to extend while allowing the garment to redistribute around the growing structure. The expansion of the hanger was therefore distributed over several smaller mechanical movements instead of being imposed primarily through a single large shoulder rotation.

Only after the telescopic and side-support mechanisms had completed their deployment were the main arms rotated through the remaining 15°, from 60° to their final 75° position. This final movement completed the shoulder expansion and established the intended supporting geometry before the original left and right garment pickup grippers were released. The garment was then allowed to settle onto the expanded hanger.

The use of the intermediate 60° position should therefore not be interpreted as an independently optimized shoulder angle or as a fundamental geometric requirement of the physical hanger. It was introduced during simulation development as an effective method of reducing garment penetration and improving the stability of the cloth–hanger interaction. The main significance of the result is that the sequence of deployment, and not only the final geometry, influences successful interaction with a deformable garment.

Future physical implementation may not require the motions to be separated as strictly as in the simulation. The hanger could potentially begin opening while it is still entering the garment, and the telescopic sections could extend progressively as the garment slides across the shoulder supports. Such coordinated motion could reduce the complete cycle time. Nevertheless, the sequential 60°–extension–15° strategy used in the simulation provides a conservative demonstration that the compact insertion state can be successfully transformed into the final expanded supporting state without directly commanding the mechanism to its maximum dimensions.

Overall, the full-cycle simulation demonstrated that the individual design decisions developed throughout the study can operate as a connected process. The front and back grippers reduced uncertainty in neckline configuration, the compact insertion geometry enabled

entry through the garment opening, and the staged deployment transformed the hanger into the larger geometry required for final garment support. The results therefore show that successful automated hanging depends not on a single optimized hanger shape, but on the coordinated relationship between garment preparation, insertion geometry, final supporting geometry, and deployment sequence.

5.8 Discussion in Relation to Research Questions

The combined results show that automated garment hanging cannot be addressed effectively by optimizing hanger geometry, garment manipulation, or robotic motion independently. Instead, the performance of the system depends on how these elements work together. The surface-exposure study demonstrated that controlled three-dimensional support can substantially improve garment visibility, while the blind-insertion experiments showed that the geometry required for entering the neckline should remain compact and tolerant to positioning uncertainty. The pickup-variation experiments further demonstrated that the configuration of the deformable neckline strongly influences insertion reliability, which led to the introduction of temporary front and back grippers for active neckline opening. Finally, the full hanger-cycle simulation demonstrated that these individual functions could be combined into one sequence in which the garment is prepared for insertion, the compact hanger enters the neckline, and the mechanism subsequently expands into the larger geometry required for garment support. These results collectively support the Design for Automation approach adopted in this study, where mechanical geometry and controlled constraints are used to reduce uncertainty that would otherwise need to be handled through sensing and complex robotic correction.

5.8.1 Research Question 1: Surface Exposure and Observation Quality

How can hanger geometry be modified to maximize surface exposure for AI analysis?

The results demonstrate that garment surface exposure can be improved by introducing controlled three-dimensional separation between the front and rear garment surfaces. Geometry supporting the garment directly influences the formation of folds, overlapping regions, and the orientation of the textile relative to the available camera viewpoints.

The standard hanger produced the weakest performance among the investigated supporting geometries. Its relatively flat configuration allowed the front and rear garment layers to remain close together, resulting in increased self-occlusion and folds. In contrast, mannequin and inflatable geometries increased the spatial separation of the garment surfaces and consequently improved total surface visibility.

However, increasing the hanger volume did not continuously improve the overall observation result. As the garment became more volumetric, larger portions of the surface were oriented at oblique angles relative to the cameras. Although these regions remained visible, their Mean Sampling Integrity decreased. The geometry evaluation therefore identified a trade-off between increasing surface separation and maintaining favorable viewing angles.

The hybrid geometry was developed in response to this trade-off. It combined the relatively thin structure of the two-dimensional frame with a limited amount of three-dimensional depth. With four cameras, the hybrid geometry achieved a surface coverage of approximately 99.52% and an Efficiency Score of 89.06%. The same geometry achieved approximately 98.78% surface coverage using only two cameras. Increasing the camera configuration from four to six produced essentially no additional improvement in surface coverage.

These results indicate that maximizing useful garment exposure does not require maximizing the volume of the supporting geometry. Instead, a limited and controlled amount of three-dimensional separation can provide high surface visibility while maintaining favorable observation angles.

The results also demonstrate that mechanical garment presentation can reduce the burden placed on the vision system. Rather than attempting to compensate for folds and occlusion only by increasing the number of cameras, the garment can first be mechanically arranged into a more observable configuration. The hanger geometry therefore becomes part of the sensing strategy by improving the physical condition of the garment before image acquisition.

5.8.2 Research Question 2: Blind Insertion and Deployable Hanger Geometry

How can hanger geometry be modified to allow for blind robotic insertion while maintaining the garment's natural shape?

The results indicate that the conflicting requirements of hanger insertion and final garment presentation can be addressed by separating these functions mechanically. A geometry that is sufficiently large to support the garment and create three-dimensional surface separation may be difficult to insert through the neckline. Conversely, a geometry optimized only for easy insertion may provide insufficient support after the garment has been hung.

The developed concept therefore uses a reconfigurable hanger with two functional states: a compact insertion state and an expanded garment-support state. During insertion, the main shoulder arms and telescopic sections remain retracted to minimize the envelope of the mechanism. After the hanger has entered the garment, these components are deployed to establish the larger final supporting geometry.

The insertion-tip experiments demonstrated that the geometry entering the neckline could tolerate meaningful translational and rotational variation under the investigated conditions. Shape2.5 produced the widest continuous successful Y-offset interval, from −11 mm to +5 mm, while Shape2.3 successfully completed all tested X-offset conditions between −30 mm and +30 mm. Shape2.3 also tolerated rotations from −15° to +15° around the X axis and demonstrated a continuous successful range of approximately −9° to +9° around the Y axis.

These results show that the insertion geometry does not need to perfectly match the neckline position to achieve successful entry. Instead, suitable geometry can provide a degree of passive mechanical tolerance to initial positioning errors.

However, the pickup-variation experiments demonstrated that insertion geometry alone was not sufficient to eliminate uncertainty. Changes in the garment pickup points altered the resulting neckline position and shape, reducing the reliability of passive insertion. Across Shape2.3 and Shape2.5, passive direct insertion successfully completed 11 of the 18 tested geometry–pickup combinations. Position correction of the insertion tool increased this to 15 of 18 combinations.

The introduction of active neckline opening provided a more robust solution. Temporary front and back grippers mechanically separated the garment surfaces before insertion, creating a larger and more stable opening. With this operation, both insertion geometries successfully completed all nine tested pickup configurations, resulting in 18 successful geometry–pickup combinations out of 18 without individual X-direction corrections.

The full-cycle simulation subsequently demonstrated that the compact insertion configuration could be transformed into the larger garment-support configuration after entry.

The results therefore indicate that blind insertion and final garment support should not be treated as requirements for a single fixed geometry. Instead, a compact and tolerant geometry can be used during the constrained insertion stage and subsequently transformed into a larger three-dimensional structure for garment support. Together with active neckline control, this reduces the dependence on continuous visual correction of the deformable garment during insertion.

5.8.3 Research Question 3: Advantage Over the Conventional Hanger

Does a specialized hanging fixture provide significantly better surface-area exposure compared with a standard hanger?

The results provide strong numerical evidence that a specialized hanging fixture can provide substantially greater garment surface exposure than a conventional hanger.

The standard hanger consistently produced the weakest surface-exposure performance among the evaluated geometries. With four cameras, the standard hanger achieved approximately 92.42% coverage, whereas the developed hybrid geometry achieved approximately 99.52% under the corresponding camera configuration. The hybrid geometry also achieved an Efficiency Score of approximately 89.06%, compared with approximately 71.70% for the standard hanger.

The improvement is important because the difference between the two concepts is not limited to their final dimensions. A conventional hanger uses essentially the same fixed geometry during both insertion and garment support. This creates an inherent compromise. Increasing the hanger dimensions may improve garment presentation but makes entry through the neckline more difficult, while reducing the dimensions simplifies insertion but decreases the ability to separate and support the garment surfaces.

The proposed deployable hanger separates these two requirements. The mechanism remains compact during insertion and expands only after it has entered the garment. Consequently, the final support geometry does not need to be constrained by the dimensions required to pass through the neckline.

This represents an important Design for Automation feature of the proposed system. Instead of requiring one fixed component to satisfy two conflicting functions, the mechanism changes configuration according to the stage of the process.

The results therefore demonstrate that a specialized fixture can substantially improve garment surface exposure while preserving a compact geometry during the insertion operation.

5.8.4 Research Question 4: Automation Efficiency and Hanging Success

Which automation approach yields the best efficiency and success rate for garment hanging?

The results provide a partial but considerably stronger answer to this research question than was possible from the initial surface-exposure study alone.

The Efficiency Score used during the geometry evaluation describes image-observation performance and should not be interpreted as the operational efficiency or success rate of the robotic hanging process. Robotic hanging performance must instead be evaluated using measures such as successful insertion, successful deployment, complete hanging success, cycle time, and failure mode.

Within the insertion strategies evaluated in this study, active mechanical control of the neckline produced the strongest result. Passive direct insertion successfully completed 11 of

the 18 tested geometry–pickup combinations, corresponding to 61.11%. Introducing X-direction recovery increased the successful coverage to 15 of 18 combinations, or 83.33%. In comparison, active neckline opening successfully completed all 18 tested combinations, corresponding to 100% successful insertion under the investigated conditions.

This comparison is particularly important because positional recovery required different corrections for different garment configurations. Active opening achieved the higher result without requiring an individual correction for each pickup condition. Mechanically controlling the neckline therefore provided a more repeatable starting condition for blind insertion.

The final automation approach consequently combined several complementary operations:

- Initial left and right garment pickup
- Temporary active opening of the front and rear garment surfaces
- Compact blind hanger insertion
- Shoulder deployment°
- Sequential telescopic expansion
- Side-support deployment
- Release of the original garment pickup grippers

The full hanger-cycle simulation demonstrated that these operations could be combined into one continuous mechanical sequence. This confirms the feasibility of transforming the garment from its initially suspended condition into a final supported condition on the expanded hanger within the investigated simulation environment.

The staged shoulder deployment was also important for the complete cycle. Direct deployment of the main arms to the final 75° position sometimes caused the shoulder sections to penetrate the simulated garment. Dividing the motion into an initial 60° deployment, followed by telescopic and side-support extension and a final 15° shoulder movement, produced more stable garment hanger interaction. This demonstrates that automation performance depends not only on the final mechanism geometry but also on the order in which the individual mechanical operations are performed.

However, the 100% result obtained during the active-opening experiment represents insertion success under the tested pickup configurations, not the statistical success rate of repeated complete hanger cycles. The full hanger cycle was demonstrated successfully as an integrated sequence, but repeated complete-cycle trials would be required before a quantitative full-system success rate and cycle-time distribution could be reported.

Based on the experiments completed in this study, the strongest investigated approach is therefore the combination of active neckline opening, compact blind insertion, and staged deployment of the reconfigurable hanger. This approach provided the highest measured insertion robustness and was successfully integrated into the complete hanger-cycle simulation. Further repeated full-cycle testing would be required to determine its overall industrial hanging success rate and operational cycle-time performance.

5.9 Limitations of the Evaluation

The results of this study should be interpreted within the limitations of the simulation-based evaluation. The developed simulations provide a controlled environment for comparing hanger geometries, evaluating insertion tolerance, investigating garment-pickup variation, and demonstrating the complete hanger sequence. However, the behavior of a simulated deformable garment cannot reproduce all physical characteristics of a real textile.

The most important limitation is therefore the real-to-simulation gap. Cloth behavior in the simulation depends on the selected material parameters, mesh resolution, friction coefficients, collision settings, solver configuration, and numerical time stepping. These factors influence how the garment stretches, folds, slides, and reacts to contact with the hanger. Consequently, successful simulation should be interpreted as evidence that the proposed mechanical concept is feasible under the investigated conditions rather than as proof that the same performance will be obtained directly with physical garments.

5.9.1 Cloth Material Representation

A real cloth is a complex deformable structure whose behavior depends on multiple interacting material characteristics. These include fiber and yarn structure, knit orientation, anisotropic stretching, bending resistance, seams, local thickness, friction, damping, previous deformation, and variation across the garment.

The simulated garment represents these behaviors using a discretized deformable mesh together with a limited set of numerical material parameters. This provides a practical approximation for evaluating hanger–garment interaction but cannot reproduce the complete mechanical behavior of a physical knitted garment.

As a result, the exact folds, local stretching, sliding behavior, and deformation observed during the simulations should not be interpreted as exact predictions of physical textile behavior. The purpose of the garment model was instead to reproduce sufficiently realistic deformability to evaluate the relative feasibility of hanger insertion, garment opening, and mechanical deployment.

The absence of detailed seam modelling is particularly relevant. Seams can locally increase stiffness and thickness and can influence how a garment slides across the hanger or resist deformation. Such effects may become important during physical hanger deployment and should therefore be included in later experimental validation.

5.9.2 Contact and Penetration Limitations

One of the main numerical challenges observed during development was non-physical penetration between the rigid hanger components and the deformable garment.

In a physical system, a garment cannot pass directly through a solid hanger component. When contact occurs, the textile must instead slide, stretch, fold, or be displaced around the moving surface. In the simulation, however, collision and contact responses are evaluated numerically at discrete physics steps.

If a rigid component moves a sufficiently large distance between successive contact evaluations, the deformable solver may not respond quickly enough to prevent geometric intersection. This can result in numerical penetration between the garment and hanger.

This behavior was particularly noticeable during rapid shoulder-arm rotation and telescopic deployment. The initial attempt to rotate the main shoulder arms directly to their final 75° position occasionally caused the hanger geometry to penetrate the T-shirt rather than progressively redistribute the cloth around the mechanism. This behavior contributed to the introduction of the intermediate 60° shoulder position before the remaining mechanical elements were deployed.

The occurrence of numerical penetration should therefore not automatically be interpreted as evidence that the same failure would occur in a physical system. Nevertheless, it remains a useful indication that the corresponding motion creates a demanding contact condition. Such motions would require particular attention during physical testing.

5.9.3 Simplified Collision Geometry

A further limitation is associated with the collision representation of the hanger. The detailed mechanical CAD model contains small edges, transitions, narrow surfaces, and other geometric features that can create unstable local contact when interacting with a deformable mesh. Individual garment nodes may become trapped around such features, producing unrealistic deformation or numerical instability.

To reduce this problem, simplified capsule-shaped geometries were used. The smoother capsule surfaces reduced the number of small geometric discontinuities interacting with the cloth and improved contact stability during deployment.

This represents a compromise between geometric fidelity and numerical robustness. The simplified collision model reproduces the overall dimensions and motion of the hanger but does not reproduce every local surface feature of the physical mechanism.

Consequently, local garment interaction around joints, edges, and transitions may differ in a physical prototype. These regions should therefore receive particular attention during real world mechanical testing.

5.9.4 Gripping and Attachment Idealization

In the simulation, selected garment vertices can be constrained directly to a gripper attachment. Once this constraint has been established, the garment remains connected to the specified attachment unless the constraint is intentionally released.

Physical grasp is more complex. Its stability depends on factors including gripping force, friction, gripper surface material, local textile thickness, garment orientation, compliance, and relative movement between the fabric and gripper. Sliding or partial loss of the grasp may therefore occur in a real system.

The simulated attachment consequently represents a more deterministic interaction than would normally be expected during physical textile handling.

The pickup-variation study addresses one important source of uncertainty by changing the garment pickup position. However, it does not reproduce all physical grasp uncertainties, particularly slipping, variable clamping force, incomplete contact, and changes in the local fabric configuration during grasp acquisition.

The performance of both the initial left–right pickup grippers and the temporary front–back opening grippers must therefore be validated experimentally using physical textile contact.

5.9.5 Limited Garment Variation

The present evaluation was performed using restricted garment models (EU size 48 -54) and therefore does not establish that the same performance will be obtained across all upper-body garments.

Real used garments vary considerably in size, neckline geometry, textile stiffness, elasticity, thickness, construction, and condition. Garments may also contain collars, reinforced seams, prints, pockets, decorative elements, or previous permanent deformation.

The insertion-tolerance and pickup-variation experiments demonstrate robustness to controlled geometric variation within the investigated T-shirt configuration, but they do not represent the complete variability expected in an industrial used-garment stream.

The reported success rates should therefore be interpreted only within the tested simulation conditions. Generalization to different garment sizes, textile materials, and neckline types requires additional evaluation.

5.9.6 Simulation and Physical Cycle Time

The simulated full hanger cycle was intentionally executed using relatively slow and separated motions. This was necessary to maintain stable deformable body interaction and to make it possible to identify the stage at which a failure occurred.

Tested sequence should not be interpreted as the fastest possible operating strategy for a physical machine.

A physical implementation could potentially use partially overlapping movements. For example, the shoulder arms could begin opening while the hanger is still completing the insertion motion. Similarly, telescopic extension could begin while the main arms continue to rotate.

The physical sequence may therefore be closer to a coordinated combination of insertion, progressive shoulder expansion, and telescopic extension rather than a series of completely independent motions.

For this reason, the cycle time observed in the simulation should be considered a conservative experimental sequence rather than a prediction of industrial production cycle time. Determining an achievable operating speed requires physical testing with real actuators and garments.

5.9.7 Implications for Physical Validation

Despite these limitations, the full-cycle simulation reduces an important uncertainty in the proposed automation concept. Prior to the integrated simulation, it remained uncertain whether the compact insertion configuration and the expanded garment-support geometry could be connected through a mechanically executable sequence while interacting with a deformable garment.

The simulation demonstrates that this transition is achievable under the conditions investigated. It also identifies several practical areas that should be prioritized during physical prototype development.

Physical validation should therefore be investigated:

1. Real textile friction and sliding behavior
2. Gripper slip and required gripping force
3. Actuator force and torque requirements
4. Garment interaction with seams and local thickness variations
5. Achievable shoulder and telescopic deployment velocities
6. Complete physical cycle time
7. Sensitivity to garment size and material
8. Reliability of the temporary neckline-opening operation
9. Repeated deployment and mechanism durability
10. Repeatability under industrial garment variation

The simulation should therefore be interpreted as evidence of technical feasibility rather than proof of industrial reliability. It demonstrates that the proposed sequence and mechanical architecture can perform the intended operation in a controlled deformable-body environment, while the remaining uncertainty concerns how robustly, quickly, and repeatably the concept transfers to physical garments and industrial operating conditions.

6 Conclusion

This thesis investigated how Design for Automation principles can be applied to simplify the automated hanging and presentation of used upper-body garments. The central challenge identified in the study was the conflict between two geometric requirements. A compact geometry is desirable for reliable insertion through the garment neckline, whereas a larger three-dimensional geometry is desirable after insertion to separate the garment surfaces and improve their presentation for image-based analysis.

The first stage of the study demonstrated that the geometry supporting the garment has a substantial influence on surface visibility and observation quality. Conventional flat hanger geometry allowed the front and rear garment surfaces to remain close together, resulting in folds and self-occlusion. Increasing the three-dimensional separation of the garment surfaces improved visibility, although excessive volumetric expansion reduced observation quality by increasing the number of surfaces viewed at oblique angles.

This trade-off led to the development of the hybrid supporting geometry. With four cameras, the hybrid configuration achieved approximately 99.52% garment surface coverage and an Efficiency Score of 89.06%, compared with approximately 92.42% coverage and 71.70% Efficiency Score for the standard hanger. The hybrid geometry also achieved approximately 98.78% coverage using only two cameras. These results demonstrate that useful garment exposure can be improved through mechanical presentation rather than relying solely on additional camera viewpoints.

The subsequent insertion experiments showed that the geometry required for garment entry should be treated separately from the geometry required for final garment support. Screening of sixteen insertion geometries demonstrated that suitable compact geometries provide meaningful tolerance to translational and rotational positioning errors. Shape2.5 provided the widest continuous successful Y-offset range, while Shape2.3 demonstrated complete success across the tested X-offset range and was subsequently evaluated under angular variation.

However, the garment-pickup experiments demonstrated that insertion geometry alone was insufficient to compensate for all uncertainty. Variation in the initial pickup locations changed the position and configuration of the neckline. Passive direct insertion succeeded for 11 of the 18 tested geometry–pickup combinations. Positional recovery increased this to 15 of 18 combinations but required configuration-dependent corrections.

A more robust result was obtained by introducing temporary front and back grippers to actively separate the garment surfaces around the neckline. With active neckline opening, all 18 tested geometry–pickup combinations successfully completed insertion without individual X-direction corrections. This result demonstrates the value of mechanically controlling the deformable garment state before the critical insertion operation.

The complete hanger-cycle simulation then demonstrated that the individual operations could be integrated into a mechanically executable sequence. The garment was suspended, the neckline was actively opened, the compact hanger was inserted, and the hanger was subsequently expanded using shoulder rotation, telescopic extension, and side-support deployment. Dividing the final 75° shoulder deployment into an intermediate 60° position followed by the remaining 15° after telescopic and side-support deployment reduced numerical garment penetration and produced more stable cloth–hanger interaction.

Additional garment trials provided preliminary evidence that the developed mechanism is not limited to one specific T-shirt geometry. Using the same hanger dimensions and deployment sequence, viable results were obtained for the evaluated male upper-body garments approximately within EU sizes 48–54. The trials also identified important geometric limits. Smaller garments experienced greater interference during deployment, particularly garments with narrow internal dimensions, while garments with very narrow necklines could fail during the initial insertion stage.

Overall, the study demonstrates that automated garment hanging can be simplified by distributing the task across several complementary mechanical functions rather than attempting to solve garment uncertainty entirely through sensing and robotic trajectory correction. The strongest investigated configuration combined a compact insertion geometry, active mechanical control of the neckline, and a deployable hanger capable of transforming into a larger supporting structure after insertion.

The results should nevertheless be interpreted as simulation-based evidence of technical feasibility rather than proof of industrial reliability. The 100% result obtained during the active-opening experiment represents insertion success for the tested geometry–pickup combinations and should not be interpreted as a 100% success rate for repeated complete hanger cycles or for arbitrary garments. Physical validation is required before conclusions can be made regarding industrial reliability, achievable cycle time, actuator requirements, or performance across a wider used-garment population.

6.1 Future Work and Research

The next stage of development should focus on transferring the proposed concept from simulation to a physical prototype. Physical experiments are required to determine whether the garment sliding, deformation, and contact behavior observed in simulation are representative of real textiles. Attention should be given to textile friction, local seam stiffness, garment stretching, gripper slip, and the forces and torques required during shoulder and telescopic deployment.

The temporary front and back neckline-opening operation should also be investigated experimentally. The simulation uses deterministic attachments between selected garment regions and the grippers, whereas a physical gripper will depend on contact force, friction, gripper material, textile thickness, and local garment configuration. A physical study should therefore determine the minimum gripping force and contact geometry required to create a stable neckline opening without damaging or excessively deforming the garment.

A second major development area is adaptation to garment size. The different-garment trials showed that the fixed final deployment configuration was suitable for the tested male garments approximately within EU sizes 48–54 but was less suitable for smaller garments and garments with narrow internal dimensions. Future mechanisms should therefore investigate variable shoulder angles and variable telescopic extension rather than deploying every garment to the same final dimensions. Garment size or characteristic dimensions could be estimated before deployment and used to determine an appropriate final hanger configuration.

The compact insertion envelope should similarly be reduced if compatibility with garments having smaller neckline openings is required. Alternative joint arrangements, thinner insertion components, or an additional collapsing mechanism could be investigated to extend the operating range of the system.

Further simulation and physical testing should also include a broader garment population. The present study primarily considers upper-body garments with related topology. Future experiments should systematically vary garment size, material, neckline design, elasticity, seam construction, and garment condition. Repeated trials are required to establish statistically meaningful complete-cycle success rates and characteristic failure probabilities.

The motion sequence itself also provides opportunities for optimization. The sequential deployment used in the present simulation was intentionally conservative. A physical system could potentially overlap insertion, shoulder rotation, and telescopic extension so that the garment progressively slides over the expanding mechanism. Such coordinated motion may reduce cycle time and improve textile redistribution compared with completely separated movements.

Finally, the mechanical hanging system should be integrated with the downstream imaging and analysis process. The surface-coverage and observation-quality metrics used in this study describe geometric imaging conditions but do not directly measure AI inspection performance. Future work should therefore determine whether the increased garment surface exposure produced by the hybrid geometry results in measurable improvements in garment classification, defect detection, or other image-analysis tasks.

6.2 Critical Discussion

The main contribution of this work is not a single optimized hanger dimension but a different way of approaching deformable-object automation. The results indicate that part of the uncertainty normally assigned to perception and control can instead be managed through mechanical design. Active neckline opening, compact insertion geometry, and post-insertion deployment each constrain the garment at a different stage of the process.

This approach also introduces additional mechanical complexity. The proposed system requires more moving components than a conventional hanger and introduces additional temporary grippers for neckline control. The reduction in sensing and trajectory-correction requirements must therefore be balanced against the cost, reliability, maintenance requirements, and control complexity associated with the additional mechanical hardware. These factors were not quantitatively evaluated in the present simulation study.

The geometry evaluation also uses calculated surface visibility and viewing-angle quality as proxies for the suitability of the garment presentation for AI analysis. These metrics allow systematic comparison of supporting geometries, but they do not directly demonstrate improved defect-detection or classification accuracy. Consequently, the results support the conclusion that the hybrid geometry provides more favorable geometric observation conditions, rather than proving that it produces a specific improvement in AI performance.

Similarly, the experiments demonstrate tolerance to controlled translational, rotational, and pickup variation but cannot reproduce the full variation present in an industrial used-garment stream. The additional GarmentLab trials extend the evaluation beyond the original T-shirt, but they also demonstrate that the selected mechanism has a finite operating envelope. Neckline size and available internal garment width remain important constraints.

Another important consideration is the dependence of dynamic deployment behavior on the simulation model. The intermediate 60° shoulder position was introduced because direct deployment to 75° caused numerical penetration in some simulations. This does not establish 60° as the physically optimal intermediate angle. Instead, it demonstrates that the sequence and velocity of expansion influence garment interaction and that these parameters must be re-evaluated using a physical prototype.

The results therefore support the feasibility of the proposed Design for Automation strategy while also defining its current boundaries. The work establishes mechanical architecture and identifies the dominant geometric and interaction constraints, but further physical and statistical evaluation is required before the concept can be characterized as an industrially reliable automated garment-hanging system.

6.3 Generalization of the Results

Although the numerical results obtained in this study are specific to the evaluated garment models, hanger dimensions, and simulation conditions, several underlying design principles are more general.

First, the geometry required for inserting a tool into a deformable object does not necessarily need to be identical to the geometry required for supporting or manipulating that object afterward. Separating these requirements through a reconfigurable mechanism can reduce geometric compromises during design.

Second, uncertainty in deformable-object manipulation can be reduced by mechanically preparing the object before a constrained operation. In this study, active separation of the garment surfaces reduced sensitivity to variations in neckline configuration. A similar principle may be applicable to other textile-handling operations in which an opening, edge, or surface must be positioned before robotic interaction.

Third, the garment trials indicate that the developed hanger has an operating range rather than compatibility with one exact garment. The tested configuration produced viable results for several male upper-body garment assets approximately within EU sizes 48–54. However, smaller garments, narrow under bust geometries, and narrow neckline openings exposed the limits of a fixed final deployment configuration. This suggests that broader garment compatibility should be achieved through adaptable deployment dimensions rather than by searching for one fixed hanger geometry intended to fit every garment.

More broadly, the study demonstrates the potential of using mechanical constraints to reduce the configuration space of highly deformable objects. By controlling selected parts of the object and transforming the supporting geometry according to the stage of the operation, part of the complexity normally assigned to perception and high-degree-of-freedom robotic control can be transferred to the mechanical system.

The extent to which these principles can be generalized to different textile categories and industrial environments remains dependent on physical validation. Nevertheless, the results provide a foundation for further development of mechanically assisted automation strategies for deformable-object handling.

7 References

[1] "Circularity of the EU textiles value chain in numbers." Accessed: Feb. 23, 2026. [Online]. Available: https://www.eea.europa.eu/en/analysis/publications/circularity-of-the-eu-textiles-value-chain-in-numbers

[2] M. B. Ramzan, S. M. Qureshi, M. S. Habib, T. Naveed, M. Awais, and H. Jamshaid, "Evaluation of human factors on visual inspection skills in textiles and clothing: A statistical approach," *J. Eng. Fibers Fabr.*, vol. 17, p. 15589250221128115, Jan. 2022, doi: 10.1177/15589250221128115.

[3] S. Eskilander, "A Method For Product Design: DFA2".

[4] F. Gu, Y. Zhou, Z. Wang, S. Jiang, and B. He, "A Survey on Robotic Manipulation of Deformable Objects: Recent Advances, Open Challenges and New Frontiers," Dec. 16, 2023, *arXiv*: arXiv:2312.10419. doi: 10.48550/arXiv.2312.10419.

[5] R. Hoque *et al.*, "Learning to Fold Real Garments with One Arm: A Case Study in Cloud-Based Robotics Research," in *2022 IEEE/RSJ International Conference on Intelligent Robots and Systems (IROS)*, Kyoto, Japan: IEEE, Oct. 2022, pp. 251–257. doi: 10.1109/IROS47612.2022.9981253.

[6] K. Suzuki, M. Kanamura, Y. Suga, H. Mori, and T. Ogata, "In-air Knotting of Rope using Dual-Arm Robot based on Deep Learning," in *2021 IEEE/RSJ International Conference on Intelligent Robots and Systems (IROS)*, Sep. 2021, pp. 6724–6731. doi: 10.1109/IROS51168.2021.9635954.

[7] R. Molfino, M. Zoppi, E. Carca, and R. Avvenente, "A new handling system for textile/clothing industry," in *ISR 2010 (41st International Symposium on Robotics) and ROBOTIK 2010 (6th German Conference on Robotics)*, Jun. 2010, pp. 1–6. Accessed: Feb. 22, 2026. [Online]. Available: https://ieeexplore.ieee.org/abstract/document/5756839

[8] L. Twardon and H. Ritter, "Interaction skills for a coat-check robot: Identifying and handling the boundary components of clothes," in *2015 IEEE International Conference on Robotics and Automation (ICRA)*, Seattle, WA, USA: IEEE, May 2015, pp. 3682–3688. doi: 10.1109/ICRA.2015.7139710.

[9] P. R. Jeyaraj and E. R. S. Nadar, "Effective textile quality processing and an accurate inspection system using the advanced deep learning technique," *Text. Res. J.*, vol. 90, no. 9–10, pp. 971–980, May 2020, doi: 10.1177/0040517519884124.

[10] Y. Zhang, "Development of an intelligent inspection system for detecting and classifying garment defects," 2013, Accessed: Feb. 21, 2026. [Online]. Available: https://theses.lib.polyu.edu.hk/handle/200/7399

[11] "jensen-group.com/fileadmin/user_upload/Images_from_Figma/Products/Hospitality/MetriQ/MetriQ_EN.pdf." Accessed: Mar. 16, 2026. [Online]. Available: https://www.jensen-group.com/fileadmin/user_upload/Images_from_Figma/Products/Hospitality/MetriQ/MetriQ_EN.pdf

[12] H. Ha and S. Song, "FlingBot: The Unreasonable Effectiveness of Dynamic Manipulation for Cloth Unfolding," Oct. 18, 2021, *arXiv*: arXiv:2105.03655. doi: 10.48550/arXiv.2105.03655.

[13] B. Zhou *et al.*, "ClothesNet: An Information-Rich 3D Garment Model Repository with Simulated Clothes Environment," Aug. 19, 2023, *arXiv*: arXiv:2308.09987. doi: 10.48550/arXiv.2308.09987.

[14] N. Gu, R. He, and L. Yu, "DeFNet: deconstructed strategy for multi-step fabric folding tasks," *J. Text. Inst.*, vol. 116, no. 8, pp. 1779–1787, Aug. 2025, doi: 10.1080/00405000.2024.2400633.

[15] "Lobster hanger." Accessed: May 02, 2026. [Online]. Available: https://www.jensen-group.com/products/garment-finishing-technology/garment-finishing/lobster-hanger

[16] "Engineering Design Process," Science Buddies. Accessed: Mar. 17, 2026. [Online]. Available: https://www.sciencebuddies.org/science-fair-projects/engineering-design-process/engineering-design-process-steps

[17] D. C. Wynn and P. J. Clarkson, "Process models in design and development," *Res. Eng. Des.*, vol. 29, no. 2, pp. 161–202, Apr. 2018, doi: 10.1007/s00163-017-0262-7.

[18] W.-L. Huang, D. Tashayyod, A. Gandjbakhche, M. Kazhdan, and M. Armand, "A Novel Method to Improve Quality Surface Coverage in Multi-View Capture," Jul. 21, 2024, *arXiv*: arXiv:2407.15883. doi: 10.48550/arXiv.2407.15883.

[19] R. Hartley and A. Zisserman, *Multiple view geometry in computer vision*, 2nd ed. Cambridge, UK ; New York: Cambridge University Press, 2003.

[20] G. L. Nemhauser, L. A. Wolsey, and M. L. Fisher, "An analysis of approximations for maximizing submodular set functions—I," *Math. Program.*, vol. 14, no. 1, pp. 265–294, Dec. 1978, doi: 10.1007/BF01588971.

[21] C. W. M. Yuen, E. H. K. Fung, W. K. Wong, L. C. Hau, and L. K. Chan, "Application of smart system to textile industry: Preliminary design of a smart hanger for garment inspection," *J. Text. Inst.*, vol. 99, no. 6, pp. 569–580, Nov. 2008, doi: 10.1080/00405000701660160.

[22] "Garment defects classification - Seampedia." Accessed: Feb. 24, 2026. [Online]. Available: https://seampedia.com/garment-defects-classification/

[23] H. Lu *et al.*, "GarmentLab: A Unified Simulation and Benchmark for Garment Manipulation," Dec. 23, 2024, *arXiv*: arXiv:2411.01200. doi: 10.48550/arXiv.2411.01200.